

**EFFECTS OF DIFFERENT AERATION CONDITIONS ON *ISOCHRYSIS*
GALBANA (T-ISO) CCMP 1324 IN A BENCH-SCALE PHOTOBIOREACTOR**

A Thesis

Presented to the Faculty of the Graduate School

of Cornell University

in Partial Fulfillment of the Requirements for the Degree of

Master of Science

By

Kim Anne Falinski

May 2009

©2009 Kim Anne Falinski

ABSTRACT

The effects of superficial gas velocity (U_{gr}), gas entrance velocity (v), and bubble size on the growth of *Isochrysis galbana* (T-ISO) was investigated in 0.6 L photobioreactors operated with airlift pumps. Superficial gas velocities ranging from 7 to 93 mm s⁻¹ were created using a 1.6 mm diameter syringe. Four sparger diameters were used to test the effects of sparger velocities that ranged from 2.48 to 73.4 m s⁻¹. The effect of bubble size was evaluated by using two styles of air stones and an open glass pipet, which created a bubble size range of 0.5 to 5 mm. The k_La values for all experimental conditions were obtained. Cell growth increased linearly with increased superficial gas velocity and decreased with increased sparger velocity. Results indicate that smaller bubble size leads to some initial cell damage, but after time the increased gas transfer produces higher growth than larger bubbles. Two mechanisms were found to cause cell damage in *I. galbana*: increasing velocity at the sparger tip and reduced bubble size. The results show that airlift systems should be designed to mitigate hydrodynamic stress due to aeration. The implications for large-scale growth of microalgae in airlift-driven tubular reactors are discussed.

BIOGRAPHICAL SKETCH

Kim Falinski completed her B.S. in Electrical Science and Engineering at Massachusetts Institute of Technology in 2002. Prior to enrolling at Cornell University, she worked as an engineer in the semiconductor manufacturing industry, spent time as a community organizer in a small village in Nepal, and taught applied math at a boarding school in The Bahamas. Her experiences abroad motivated a degree that would address agriculture problems in the developing world.

For my beekeeping friend.

ACKNOWLEDGEMENTS

I would like to thank all those who helped me complete this work at Oceanic Institute in Waimānalo, Hawaii. Foremost is Dr. Charles Laidley, whose time, input and resources have made this project possible. Thank you for accepting me into your lab, coming from 5,000 miles away, for hands-on training in algal culture. I especially appreciate your time in helping me to understand the world of science.

For Eric Martinson, who not only helped me with the details of prepping the experiments, but was also a major sounding board for all steps of the process. Thank you for letting me carry buckets when I just needed to let my head think, and for taking me in without question when I flew onto the island with no where to stay.

For members of the Finfish Department: Iokepa Aipa, Chad Callan, Melissa Carr, Dean Kline, Ken Liu, Don de la Pena, and Kim Pinkerton – thank you for the encouragement, holiday dinners, and general cheerleading towards graduation. And thank you so much for letting me learn about how to raise fish in the process- it will be put to good use. Thanks to Lytha Conquest, Dr. Carrie Holl and Dr. Z.Y. Ju for their assistance with lab techniques and equipment. And to Tom Ogawa, thank you much for all that coffee.

For Willow Hetrick – whose apartment has been my grad school away from home. You are inspiring in your perseverance and I hope to be half as effective as you someday in getting things done.

For my best friend Howard McGinnis. Thank you so much for everything.

As for the other side of the world, here are my East Coast thanks: For my parents – thank you for the solid base I am now standing on. You never really complained when I decided to go into a very different field halfway around the world.

For Dr. Neema Kudva. Your seminar class in 2006 was why I decided to stay in the colds of Ithaca, in an engineering degree, and have helped me to interpret the

always complex web of relationships between non-profit organizations and government.

For Dr. Len Lion – chemistry has been the base of what I have done and I thank you for your diligence in teaching me the carbonate system. You were one of the first to have faith in me in this field.

And, lastly, for my advisor Dr. Michael Timmons, who has guided me through this degree with patience. I truly appreciate you letting me figure out things the long way, and for getting me to a place where I could really learn.

TABLE OF CONTENTS

BIOGRAPHICAL SKETCH	iii
DEDICATION	iv
ACKNOWLEDGEMENTS	v
LIST OF FIGURES	viii
LIST OF TABLES	ix
LIST OF SYMBOLS	x
1. Introduction	1
1.1. <i>Isochrysis galbana (T-ISO)</i>	1
1.2. <i>Large-scale photobioreactor systems</i>	2
1.3. <i>Airlift systems</i>	3
1.4. <i>Turbulence as the key issue in photobioreactor systems</i>	4
1.5. <i>Methodologies for determining shear stress in bioreactors</i>	8
1.6. <i>Objective</i>	10
2. Materials and Methods	11
2.1 <i>Theory and analysis</i>	11
2.1.1. <i>Statistical analyses</i>	11
2.1.2. <i>Superficial gas velocity</i>	11
2.1.3. <i>Sparger velocity</i>	12
2.1.4. <i>Growth kinetics</i>	12
2.1.5. <i>Determining the k_La</i>	13
2.1.6. <i>Design of the model airlift system</i>	14
2.2. <i>Microalgae and culture media</i>	14
2.3. <i>Cultivation system: experimental mini-airlift</i>	15
2.4. <i>Analytical methods</i>	18
2.4.1. <i>Cell density and viability</i>	18
2.4.2. <i>Measurements</i>	19
2.5. <i>Experiments</i>	19
3. Results and Discussion	21
3.1. <i>Effects of superficial gas velocity</i>	21
3.2. <i>Effects of sparger velocity</i>	26
3.3. <i>Effect of gas diffusers</i>	31
3.4. <i>Implications for airlift-driven tubular photobioreactors</i>	39
3.5. <i>Design Example</i>	42
4. Conclusion	45
APPENDIX A	46
APPENDIX B	47
APPENDIX C	48
REFERENCES	49

LIST OF FIGURES

Figure 1.1: Five different types of air-driven reactors.....	4
Figure 2.1: Schematic drawing of the airlift bench-scale photobioreactor.....	16
Figure 2.2: Photograph of the experimental setup of bench-scale internal airlift bioreactors.....	18
Figure 3.1: Effect of superficial gas velocity in the riser, U_{gr} , on the cell density of <i>I. galbana</i> at 120 hours.....	22
Figure 3.2: Growth curve of <i>I. galbana</i> grown in batch culture at different superficial gas velocities.....	22
Figure 3.3: Growth rates of <i>I. galbana</i> cultured at different superficial gas velocities.....	23
Figure 3.4: Mass transfer coefficient, k_{La} , as a function of superficial gas velocity in the riser, U_{gr}	24
Figure 3.5: Effects of increased sparger velocity on the cell density of <i>I.</i> <i>galbana</i> at 120 hours.....	27
Figure 3.6: Growth rates of <i>I. galbana</i> cultivated at different sparger velocities.....	27
Figure 3.7: Mass transfer coefficient, k_{La} , for spargers ($n=1$) as a function of sparger velocity.....	29
Figure 3.8: Effects of three different sizes of bubbles on <i>I. galbana</i> over the first 24-hour period in a bench-scale split-cell photobioreactor.....	32
Figure 3.9: Growth rates of <i>I. galbana</i> cultured with different diffuser types.....	34
Figure 3.10: Final cell densities and pH for each of the diffuser configurations.....	35
Figure 3.11: Mass transfer coefficients, k_{La} , measured for different types of diffusers.....	36

LIST OF TABLES

Table 3.1: Maximum specific net growth rate as affected by air flow and gas velocity.....	21
Table 3.2: Experimental conditions for sparger velocity experiments.	26
Table 3.3: Results of an LSD post-hoc test on sparger velocity data.	28
Table 3.4 Typical values needed for 35 m s ⁻¹ liquid velocity in airlift-driven tubular photobioreactors.	42

LIST OF SYMBOLS

A_r	cross-sectional area of the riser [m^2]
A_d	cross-sectional area of the downcomer [m^2]
C_f	Fanning friction factor []
C_X	cell concentration [cells mL^{-1}]
C_L	oxygen concentration [$kg\ m^{-2}$]
C^*	equilibrium oxygen concentration [$kg\ m^{-2}$]
d_i	nozzle internal diameter [m]
d_b	bubble diameter [m]
F_g	gas flow rate [$m^3\ s^{-1}$]
f	bubble generation frequency [s^{-1}]
g	gravitational acceleration [$m\ s^{-2}$]
h	culture height [m]
k_d	cell death rate [h^{-1}]
k_{La}	mass transfer coefficient [h^{-1}]
l	tubular photobioreactor tube length
n	number of nozzles [-]
P_h	pressure in the head zone [Pa]
Q_m	molar flow rate [$mol\ s^{-1}$]
r	column radius [m]
Re	Reynold's number []
t	time [h]
T	temperature [K]
U_L	liquid velocity [$m\ s^{-1}$]
U_g	superficial gas velocity [$m\ s^{-1}$]
U_{gr}	superficial gas velocity in the riser [$m\ s^{-1}$]
V	culture volume [m^3]
X_t	cell concentration [cells mL^{-1}]

Greek symbols

Δh	head loss [m]
η	dynamic viscosity [Pa s]
λ	microeddy length [m]
μ	specific net growth rate [h^{-1}]
μ_{max}	maximum specific net growth rate [h^{-1}]
v	sparger velocity [$m\ s^{-1}$]
ξ	specific energy dissipation [$J\ s^{-1}\ kg^{-1}$]
ρ	liquid density [$kg\ m^{-3}$]
φ	tube diameter [m]

1. Introduction

The production of a constant supply of microalgae is often identified as one of the most important technical limitations of the aquaculture industry (Richmond, 1993; Borowitzka, 1996; Pulz, 2001). Live microalgae are the primary food source for the larval stages of many fish, shellfish and crustaceans (Mueller-Fuega, 2000; Wikfors and Ohno, 2001). A significant body of research has been dedicated to the development of cost effective and reliable methods of culture in enclosed photobioreactors, yet large-scale microalgal culture continues to rely heavily on outdoor raceway ponds (Chisti, 2007). Outdoor open cultures can be maintained in large volumes, but limited light penetration, susceptibility to temperature fluctuations and contaminants limit growth rate and cell density. While researchers have offered results showing high cell densities in closed small-scale reactors (Weissman, 1987; Qiang, 1994), scale-up to sufficient volumetric capacity for the aquaculture industry has not been shown successfully to date.

1.1. Isochrysis galbana (T-ISO)

The use of the flagellated haptophyte *Isochrysis galbana* (Ewart, 1981) has been widely used in marine finfish, shellfish and shrimp hatcheries. The Tahitian species *I. galbana* (T-ISO) has been identified as an important first feed for zooplankton and larval fish and a good source of polyunsaturated fatty acids like eicosapentaenoic acid (EPA) and docosahexaenoic acid (DHA) (Kaplan, 1986; Benemann, 1992; Gladue and Maxey, 1994; Borowitzka, 1996). It has replaced the species *I. galbana* Parke for use in tropical aquaculture because of its moderate growth, even at temperatures as high as 30°C (Nelson, 1992; Tzovenis et al., 2003).

The *I. galbana* (T-ISO) cells have been found to have no distinct cell wall and only possess a plasma membrane (Zhu, 1997; Liu and Lin, 2001). Species lacking cell

walls generally are more susceptible to hydrodynamic stress (Merchuk, 1991), yet studies for *I. galbana* have not been conducted to establish the species' tolerance to aeration related stress. Cells are generally solitary, motile, and ellipsoidal in shape: 5-6 μm long, 2-4 μm wide, and 2.5-3 μm thick. There are two smooth flagella that are about equal in length, approximately 7 μm long. The cells are inserted with abbreviated haptonema (Liu and Lin, 2001).

1.2. Large-scale photobioreactor systems

For applications requiring a constant axenic supply of algae, it is essential to use enclosed photobioreactors in which monocultures can be maintained for an extended time period. Photobioreactors are defined as per Tredici (1999), as reactors that do not allow direct exchange of gases or contaminants between the culture and the atmosphere. Stability is sought by regulating all biologically important parameters, including carbon dioxide, pH, oxygen, nutrients and light.

John Pirt et al. (1980) were the first to document a tubular bioreactor for the production of *Chlorella*. The topic of photobioreactors has been reviewed by a number of authors, most notably Borowitzka (1996), Tredici (1999), Pulz (2001) Richmond (2004), Janssen et al. (2002), and in addition to the classic document by Burlew (1953).

Several types of geometries for closed reactors have been introduced that are classified by Tredici (1999) as (1) flat or tubular; (2) horizontal, inclined, vertical or spiral; and (3) manifold or serpentine. Reactors may also be considered based on their lighting source, whether solar or artificial, internally versus externally illuminated, constant or flashing light source and by the pumping mechanism, either airlift or electric pump.

Within this range of configurations, modern reactors are primarily designed as serpentine tubular photobioreactor (Pirt, 1983; Chaumont, 1993; Molina, 2001) using plastic tubes or plastic bags ranging from 2.5 to 30 cm in diameter. Also used, but less common are manifold photobioreactors (Lee et al., 1995; Babcock et al., 2002), helical photobioreactors (Watanabe and Hall, 1996), vertical photobioreactors (both airlift and bubble) (Sanchez-Miron et al., 2000; Xu et al., 2002; Krichnavaruk et al., 2003), and flat bioreactors, including alveolar panels (Tredici et al., 1991; Richmond and Cheng-Wu, 2001; Degen et al., 2001; Goksan et al., 2003).

For the type of studies pursued in this paper, an airlift-driven tubular serpentine bioreactor is the most commonly used closed photobioreactor. This type of bioreactor offers a comparatively simple design that requires less pumping capacity than a tubular manifold reactor, may use off-the-shelf parts for construction, and simplifies monitoring and evaluation. Chisti (2007) recommended tubular serpentine reactors as the most likely type of reactor to be successful at mass culture of microalgae.

1.3. Airlift systems

Design considerations for airlift bioreactors have been described extensively (Chisti, 1988; Merchuk, 1999; Acien-Fernandez et al., 2001). An airlift pump operates by injecting air into the bottom of a reactor, displacing the culture and creating a pressure differential that moves the culture in the direction of the rising bubbles. An airlift system has two main variables that can be used to characterize the flow: the superficial gas velocity, U_g , (the rate at which the bubbles rise) and the liquid flow rate (variables are defined in the Materials and Methods Section).

There are five types of air-driven reactors, as categorized by shape, as shown in Figure 1.1.

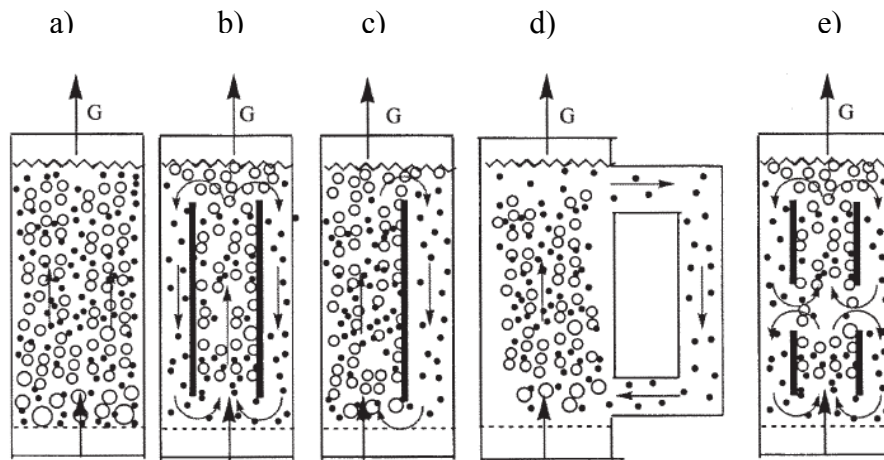


Figure 1.1: Five different types of air-driven reactors: a) bubble reactor b) concentric airlift c) internal split-cell airlift d) external airlift e) double cell airlift (Petersen and Margaritis, 2001)

The geometry of an airlift includes a riser, or section of the airlift where the bubbles are rising, and a downcomer, where the culture media again returns towards the bottom. The distance between the inner baffle and the bottom affects the velocity of the liquid, as does the area of the riser and downcomer. The amount of pressure head in the system also affects liquid velocity and should be kept small in comparison with the height of the airlift. Another parameter of importance in designing the liquid velocity is the gas holdup, or percentage, by volume, of air within the air-liquid system. Airlift reactors can be in three different phases which affect the gas velocity and liquid flow rate, based on the sizes of the bubbles: slug flow, bubbly-slug flow and bubbly flow. The effect of the different regimes on the health of algae cells has not been reported.

1.4. Turbulence as the key issue in photobioreactor systems

The most pressing issues in large-scale photobioreactor design involve how to maintain sufficient levels of mixing to maximize light-dark cycling and light availability, prevent cells from settling, prevent dissolved oxygen build-up above toxic

levels, and disperse heat without damaging temperature-sensitive algae cells (Gudin, 1991; Tredici, 1999, p. 21; Molina-Grima et al., 2000; Acien-Fernandez, 2001; Chisti, 2007). Mixing also minimizes gradients in temperature and nutrients and increases gas and light transfer.

Light-dark mixing frequencies on the order of seconds have been found, experimentally, to be necessary for optimal biomass production and growth rates (Lee and Pirt, 1981; Grobelaar, 1989; Janssen, 2003; Park, 2001). The process has also been modeled by researchers to understand further the influence of mixing on cell growth rate (Acien-Fernandez et al., 1997; Wu and Merchuk, 2001). Results indicate that increased mixing by aeration contributes positively to cell growth.

Shearing action in sparged photobioreactors is a necessary byproduct of mixing. Cell damage resulting from shear stress has been referred to as the key problem to be reduced if photobioreactors are to be successfully used for culturing microalgae (Gudin, 1991; Pulz, 2001). Although the growth rates of many microalgae have been shown to increase initially with increased aeration due to the improved supply of CO₂ and more frequent access to light, shear damage due to aeration has been shown for many species to result in reduced cell production (Silva et al., 1987; Contreras et al., 1998; Chisti, 1999; Barbosa, 2003b).

Shear damage has been studied extensively in other types of cells that are mass cultured for pharmaceutical and bioengineering purposes, such as plant (Silva et al., 1987; Moo-Young and Chisti, 1988; Gong, 2003), animal (Arathoon and Birch, 1986; Zhang, 1995), insect (Tramper and Vlak, 1989) and microbial (Edwards, 1989; Lange, 2001; Sahoo, 2003) cells. Similar to algal culture, culture of plant, animal and insect cells at larger scales also places cells in liquid media in a bioreactor. Mammalian and plant cells in culture are comparatively more susceptible than microorganisms, due to their typically larger size (Merchuk, 1999). Excessive shear, specifically in the form of

aeration, has also been shown to lead to impaired cell growth, cell damage and eventually cell death in many different microalgae species including *Dunaliella* (Silva, 1987; Barbosa, 2004), *Haematococcus* (Vega-Estrada, 2005), *Gymnodinium splendens* (Thomas et al., 1990), *Skeletona constatum* (Vandanjon et al., 1998), *Phaedactylum tricorutum* (Contreras et al., 1998; Garcia-Camacho et al., 1999; Sanchez-Miron et al., 1999; Sanchez-Miron et al., 2003; Brindley-Alias et al., 2004), *Spirulina platensis* (Bronnenmeier, 1981) and *Tetraselmis* (Jaouen, 1998).

Shear damage, hydrodynamic stress and turbulence can affect the performance of closed tubular bioreactors. High rates of flows through tubular photobioreactor tubes are needed to maintain a high level of mixing. Some researchers have reported that cultures risk collapse when liquid velocity in photobioreactor tubes falls below 35 cm s⁻¹ (Hu and Richmond, 1994; Acien-Fernandez, 1999). The type of pump used to circulate the culture may be a primary source of shear damage. The use of centrifugal pumps, specifically, has been shown to negatively impact growth of some species of algae (Gudin and Chaumont, 1991; Vandanjon, 1998; Chisti, 1995; Jaouen, 1999; Mercuk et al., 2000, Sanchez-Perez, 2006). Some researchers have used static baffles to increase mixing within the tubes (Ugwu, 2002), but this approach is difficult to scale up to many tubes of small diameters due to manufacturing costs and cleaning and maintenance issues.

Tubular bioreactors may alternatively utilize airlift pumps to mitigate shear damage from mechanical pumps. Gudin and Chaumont (1991) determined that replacing mechanical pumps with airlift systems increased productivity up to 75%. The main advantage of airlift-driven reactors is that shear distribution is more homogenous throughout the reactor than mechanical pumps and stirred tank reactors, which minimizes cell damage (Petersen, 2001). Microalgae cells, however, are not entirely immune to the damaging effects of air-induced hydrodynamic stress. High

sparger velocities, air flow rates and decreased bubble size, amongst others, have been shown to reduce cell growth (Barbosa, 2004; Vega-Estrada, 2005).

In airlift systems, the main energy input, and therefore the largest source of shear, is the velocities created by the pneumatic input of the gas into the lifting column (Sanchez-Perez et al., 2006). Contreras et al. (1999) determined that the largest fraction of the total energy expended dissipates in the riser. The percentage of energy dissipated by the separator, downcomer, and cylinder bottom is small by comparison, but remains a consideration based on the geometrical configuration of the airlift reactor. For example, if the distance between the separator and the bottom is too small, then the algae cells will be more likely to collide with the bottom as they make the 180° turn into the riser. If the separator is rough on the edges and the airlift is small, it is possible that the friction can cause damage to the algae cells.

The average shear rate has been shown to depend on the superficial gas velocity (Sanchez-Perez et al., 2006), sparger velocity (Barbosa, 2003), bubble size and column height (Garcia-Camacho et al., 2000). Three regions in a bubble column have been identified as places where cell damage might occur: (1) within the column as the bubbles rise, (2) at the sparger orifice and (3) at the surface where the bubble breaks (Molina-Grima et al., 1997; Barbosa, 2003). These three areas can also be associated directly with the superficial gas velocity, the sparger orifice velocity, and the bursting rate at the surface as represented by the bubble size, respectively (Wang et al., 1994).

Some researchers have suggested that within airlift reactors which have central baffles, contact with the baffle may also induce damage. Yet others have considered the role of the reactor height (Garcia-Camacho et al., 2000; Barbosa, 2003b). A very tall reactor would have a higher pressure at the bottom than at the top, creating a differential pressure which might cause cell damage. Bubble sizes also change as the bubble rises through a tall column, getting larger towards the top (Barbosa, 2003a).

The larger size bubble could then increase cell damage when bubble rupture occurs at the column surface. This study chose to focus on the effects of air flow without modifying the height of the column, thereby eliminating column height as a variable. The height, however, may still have a role in hydrodynamic stress.

Microeddies in tubular photobioreactors have also been identified as an important source of hydrodynamic stress for microalgae cells (Sanchez-Miron et al., 1999). Cell dimensions have to be approximately equal to or less than the calculated microeddy length for the microeddies to become significant sources of stress (Sanchez-Miron et al., 1999). Using Kolmogoroff's theory of local isotropic turbulence (Kawase and Moo-Young, 1990) as described by Acien-Fernandez et al. (2001), it can be shown that the microeddy length is inversely proportional to the liquid velocity (see Appendix A for the calculations of microeddy length). The author calculated that for a 5 cm diameter tube with liquid velocity 50 cm s^{-1} , a higher velocity than is typically used for tubular bioreactors, the microeddy length is approximately $75 \text{ }\mu\text{m}$, substantially larger than the diameter of an *I. galbana* (T-ISO) cell. As a result, in this work microeddies were not considered to be a significant source of shear stress for *I. galbana*.

There has been limited or no research on macroeddies, which are on a scale similar to the diameter of the column. It is possible that these eddies within the column may cause shear stress in the microalgae, but their potential impact was not considered in the present study.

1.5. Methodologies for determining shear stress in bioreactors

Researchers have found that hydrodynamic conditions that were used in bench-scale conditions could not be used to predict the behavior of pilot-scale systems, although similar spargers and gas velocities were used (Camacho et al., 2001).

Because it is unknown which parameters can be applied directly to design scale-up, stresses due to hydrodynamic conditions should be categorized in as many ways as possible. Future research focused specifically on scale-up issues may then benefit from previous studies of microalgal tolerance to hydrodynamic stress. There are numerous indicators used to characterize shear sensitivity. Amongst the different units used to compare turbulence and shear, researchers have used rotational speed (Jaoen, 1999), Reynold's number (Gudin, 1991; Suzuki, 1995), volumetric gas flow (Vega-Estrada et al, 2003), gas velocity (Barbosa, 2003a), agitation speed (Sobczuk et al., 2006), pressure drop coefficient (Vandanjon et al., 1998) and energy dissipation rate (Kresta, 1998).

A number of different methods and types of experimental equipment have been used to measure the effects of shear stress and shear rate on microalgae cells, plants cells and animal cells. Several studies have attempted to characterize shear tolerance of algal cultures in stirred tank photobioreactors (Wang et al., 1994), while others have used shake tables. Microalgal production in batch, bench-scale, and split-cell airlifts is an effective way to examine the tolerance of a species to air-induced stress (Vega-Estrada et al., 2005). Split-cell airlifts are columns with an internal baffle that creates two "cells". Split-cell reactors allow for easy calculation of gas velocity, liquid velocity, and gas holdup in the culture (Chisti, 1995). Through minimal changes in internal geometry and airflow in airlift bioreactors, it is possible to change the superficial gas velocity, sparger velocity, oxygen transfer rates, liquid velocity and frequency of light exposure, and to calculate these variables for comparison with other systems.

1.6. Objective

The objective of the present work is to establish aeration conditions that inhibit growth rates of *I. galbana* (T-ISO) and to extrapolate this information to guide the engineering design of production scale tubular photobioreactors.

2. Materials and Methods

An inexpensive 0.6 L split-cylinder internal-loop airlift photobioreactor was designed and assembled, as described below, based on design of Vega-Estrada et al. (2005) to evaluate the effects of shear as induced by aeration processes. Using these cylinders, batch experiments were conducted to evaluate final density and growth rate of *I. galbana* (T-ISO) as affected by superficial gas velocity in the riser (U_{gr}), gas entrance velocity (v) and bubble size.

2.1 Theory and analysis

2.1.1. Statistical analyses

Data were treated statistically by one-way analysis of variance (ANOVA) using SPSS (Version 16). When the ANOVA results were significant, a Fisher's Least Significant Differences (LSD) post-hoc test was done to verify results between groups. Regression was performed with linear least squares regression.

2.1.2. Superficial gas velocity

For the lab-scale airlift reactors, superficial gas velocity was calculated according to Eq. 2.1,

$$U_g = \frac{F_g}{A} \quad \text{Eq. 2.1}$$

where F_g is the volumetric gas flow rate ($\text{m}^3 \text{s}^{-1}$) and A is the cross-sectional area. Given the experimental setup described above, the superficial velocity was calculated using only the area of the riser.

For comparisons to the manifold bioreactor, the superficial gas velocity was calculated according to Eq. 2.2, which corresponds to the height-averaged superficial gas velocity.

$$U_g = \frac{Q_m RT}{h_a A \rho g} \ln \left(1 + \frac{\rho g h_d}{P_h} \right) \quad \text{Eq. 2.2}$$

where Q_m is the molar flow rate of the gas, h_d is the static height of the free liquid, R is the gas constant, T is temperature (K), A is the cross-sectional area of the column and P_h is the pressure in the head zone (Pa) (Barbosa, 2003).

2.1.3. Sparger velocity

The sparger velocity, or gas entrance velocity, v , was calculated according to Eq. 2.3 for experiments that used spargers:

$$v = \frac{F_g}{n * \frac{1}{4} \pi d_i^2} \quad \text{Eq. 2.3}$$

where d_i is the diameter of the nozzle, n is the number of nozzles used (in this paper there was only a single nozzle) and F_g is the volumetric gas flow rate ($\text{m}^3 \text{s}^{-1}$). No estimate of sparger velocity was made for the bubble size experiment. For purposes of comparison with other authors, the Reynold's number (Re) at the orifice was also used to assess the magnitude of the air flow at the sparger tip. Re was calculated according to Silva (1987), modified for an increased number of nozzles, as follows:

$$\text{Re}_{OL} = \frac{4\rho F_g}{n * d_i \eta} \quad \text{Eq. 2.4}$$

where ρ is the liquid density (kg m^{-3}), F_g is the gas flow rate, and η is the liquid dynamic viscosity ($\text{kg s}^{-1} \text{m}^{-1}$).

2.1.4. Growth kinetics

The cell growth rate can be described by Monod kinetics:

$$r = \frac{dX_t}{dt} = \mu X_t \quad \text{Eq. 2.5}$$

where r is the cell growth rate; C_X is cellular density and μ is the specific net growth rate.

The specific net growth rate (μ) was determined from the slope of the growth curve of cells. In the batch experiments, the lag phase was less than 24 hours and therefore neglected in calculations of μ , unless otherwise noted. By integration from t to t_0 and simplification of Eq. 2.5, μ was calculated as:

$$\mu(t) = \frac{\ln\left(\frac{X_t}{X_o}\right)}{(t - t_0)} \quad \text{Eq. 2.6}$$

In the calculations used in this paper, X_0 was taken as the inoculation density, 4×10^6 cells mL^{-1} . The maximum growth rate (μ_{max}) was calculated at 48 hours, when the growth rate was highest throughout all experimental conditions and trials. Doubling time, t_d , is defined as the amount of time needed for the biomass to double:

$$t_d = \frac{\ln 2}{\mu} \quad \text{Eq. 2.7}$$

2.1.5. Determining the $k_L a$

The overall oxygen mass transfer coefficient, $k_L a$, was determined by the dynamic gassing-in method as outlined by Chisti (1989) and Petersen and Margaritis (2001). A multi-probe YSI instrument, with a steady-state polarographic electrode, was used to record inline dissolved oxygen every one second. The probe was calibrated to air saturation prior to all experiments. Using a single mini-airlift reactor, salt water (20°C , 31 ± 1 ppt) was first sparged with nitrogen to remove dissolved oxygen, and then connected to the air source. The YSI was inserted from the top of the open mini-airlift

reactor. The $k_L a$ was then calculated according to the ASCE Standard 2-91 (ASCE, 1992) as follows:

$$\frac{dC_L}{dt} = k_L a (C_L - C^*) \quad \text{Eq. 2.8}$$

where C^* is the saturation concentration of dissolved oxygen in the reactor vessel water and C_L is the concentration in the liquid. The model assumes a perfectly mixed system. Only values of C_L between $0.5 C^*$ and C^* were used for the regression in order to minimize the impact of inaccurate readings of C_L , which would be the largest during the beginning of a gas transfer test and slow probe response.

The mass transfer coefficient for carbon dioxide, $k_L a[\text{CO}_2]$ has been shown to be approximately 0.8 to 0.9 of the $k_L a$ for oxygen, depending on the alkalinity and temperature of the water, thereby providing a means to establish relative carbon dioxide mass transfer, as well (Talbot et al., 1991; Aitchinson et al., 2007).

2.1.6. Design of the model airlift system

Data was obtained for the model large-scale tubular bioreactor airlift system using the airlift software module provided by Timmons and Ebeling (2007) in *Recirculating Aquaculture*.

2.2. Microalgae and culture media

The marine microalgae *Isochrysis galbana* (T-ISO) CCMP 1324 (to be referred to as *I. galbana*) was obtained from the collection of the Provasoli-Guillard National Center for Culture of Marine Phytoplankton, West Boothbay Harbor, Maine, USA. The inoculum for the experiments was grown indoors in 2 L Erlenmeyer flasks aerated at approximately one vvm¹. Cultures were transferred into experiments in late log-

¹ The unit 'vvm' is used for bioreactor culture. The first 'v' stands for volume of air (e.g. liter) ; the second 'v' stands for per unit of medium (e.g. liter); 'm' stands for per unit of time (e.g. minute). For example, 2 vvm (l/l/m) means in 1 minute time there is 2 liters of air passing through 1 liter of medium.

phase of growth, usually on day 7 or 8. Culture vessels were maintained in artificial 24-hour light provided by 14 white florescent bulbs (32W, Sylvania), measured at $240 \mu\text{Em}^{-2} \text{ s}^{-1}$ light flux at the vessel's surface using a 2π PAR sensor (QSL-100, Biospherical Instruments, San Jose, CA). The microalgae was cultivated using an f/2 medium as described by Guillard and Ryter (1962) (see Appendix B for details of composition) at a constant room temperature of $20^\circ\text{C} \pm 1^\circ\text{C}$ and salinity 31 ± 1 ppt. The pre-culture medium was identical to that used in the experimental cultivation, with the exception that flasks were autoclaved (120° , 45 min) while the airlift vessels were bleached (0.1% v/v, 35% bleach) prior to addition of media.

2.3. Cultivation system: experimental mini-airlift

Sixteen identical mini-airlifts of working volume 600 mL were constructed based on the design of Vega-Estrada (2005) (Figure 2.1).

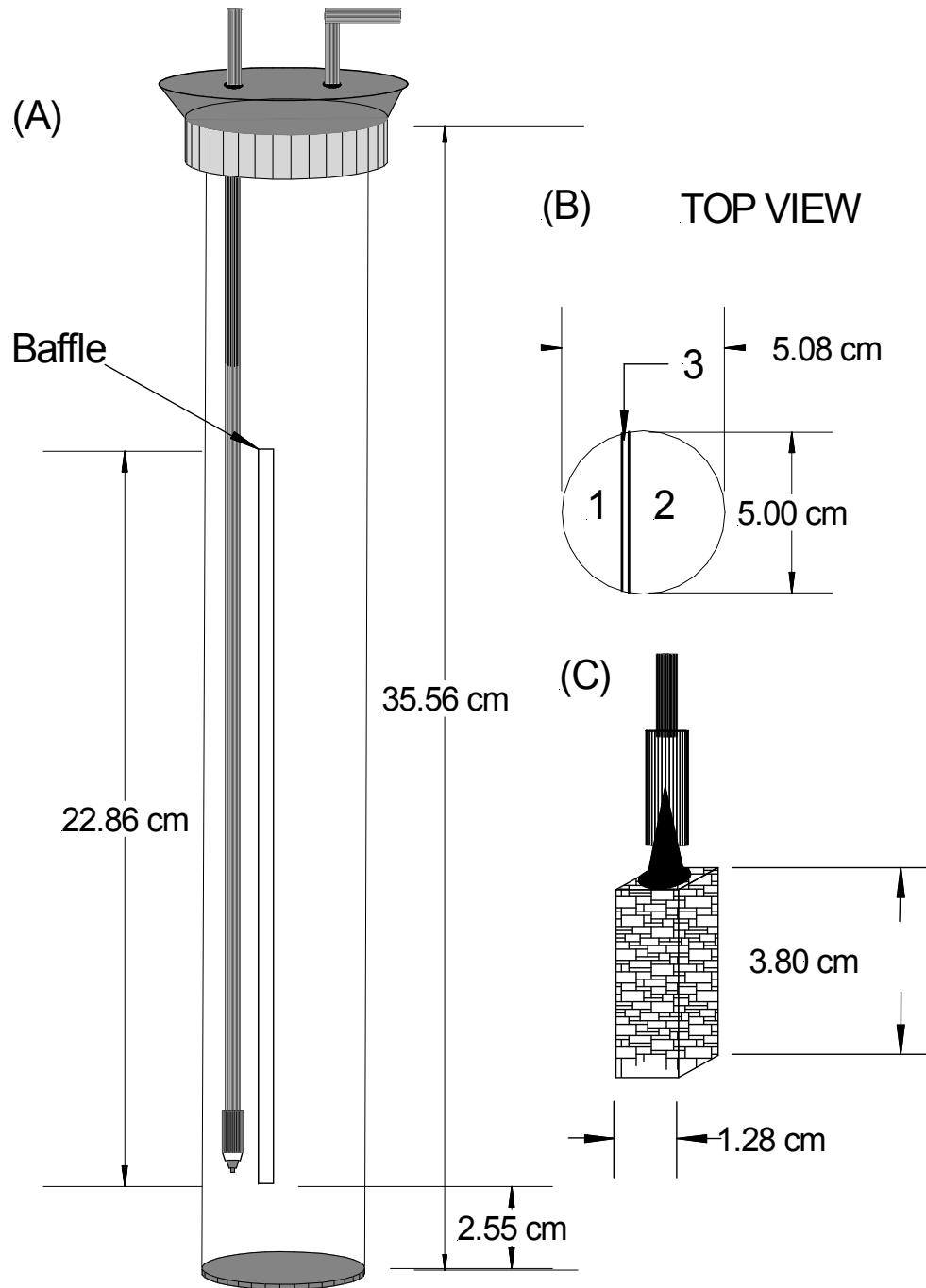


Figure 2.1: Schematic drawing of the airlift bench-scale photobioreactor. (A) Size 13 stopper with holes for 3.2 mm glass pipets for air inlet and outlet. Configuration shown includes the syringe tip with attachment space for a needle. The cylinder was made of clear Harvel™ PVC. The 0.32 cm clear internal baffle is labeled. (B) Top view of cylinder, showing dimensions of the baffle, allowing for $A_r/A_d = 0.5$. (1) riser, (2) downcomer (3) baffle. (C) Configuration of the air sparger assembly to be placed at the end of the glass pipet.

A rubber stopper (size 13) with two holes and a glass tube (3.2 mm diameter) was used as an air outlet. The cylinder was constructed of clear 5.08 cm diameter Harvel™ PVC, with a plastic end-cap as a base. A vertical clear acrylic baffle (22.9 cm x 5 cm x 0.32 cm) split the riser from the downcomer while allowing light to pass through. The liquid was mixed by sparging air in the reactor bottom through a plastic syringe that had been modified to fit onto the glass pipet. The luer lock connector allowed easy interchange between different stainless steel needle sizes. The luer lock connector without a needle was 1.6 mm diameter. The sparger tip was placed equal to the bottom of the baffle, facing downward, in the middle of the riser. The riser/downcomer cross-sectional area ratio (A_r/A_d) was 0.5, the bottom clearance was 2.54 cm, and the depth of liquid was 25.4 cm. The cylinder provided a total illuminated surface area of approximately 163.3 cm², located perpendicular on a single side of the cylinder (more details of the photobioreactor are given in Figure 2.1). Cylinders were placed 5 cm apart from one another as seen in Figure 2.2. A 0.2 μm air filter was used to filter the incoming air supplied by a pressurized air source (~3 psi). Each airlift was able to be disassembled to be disinfected separately, with the exception of the baffle, which was permanently attached to the PVC cylinder using Marine 5200 glue. The approximate materials cost of each cylinder was less than \$10.00.



Figure 2.2: Photograph of the experimental setup of bench-scale internal airlift bioreactors. The vertical line on each cylinder is the profile view of the baffle.

2.4. Analytical methods

2.4.1. Cell density and viability

Cell counting was done in duplicate every 24 hours in an improved Neubauer hemacytometer (Aquatic Ecosystems, USA) under an optical microscope using 1 mL of sample. When the cell density was greater than 25×10^6 cells mL^{-1} , the sample was diluted for more accurate assessment. For cultures with the slowest growth rates, cell viability was assessed by the Trypan blue dye exclusion method (Crippen and Perrier, 1974). Thus, 0.2 mL of microalgal suspension was diluted with 0.3 mL of sterile saline (NaCl, 9% (w/w)) and mixed with 0.5 mL of Trypan blue solution (0.4% (w/v)) (Sanchez-Miron et al., 2003). The mixture was held for 15 minutes. Non-viable cells took up the blue dye. The live and dead cells were counted in the hemacytometer to calculate the percentage of the viable cells.

2.4.2. Measurements

Salinity and pH were measured with a Yellow Springs Instruments 556 Multiprobe System (YSI) (Yellow Springs, CO, USA) at the beginning and end of each experiment. The calibration of the YSI was checked weekly. Experiments were considered complete if pH reached greater than 9.0, which had been previously established as the pH where the culture enters a stationary phase. Air flow was calibrated daily using an in-line air flow meter (MFR5 and MFR40, Key Incorporated Instruments, Treviso, PA).

2.5. Experiments

All cultures were inoculated at 16% (v/v), or 4×10^6 cells mL⁻¹, unless otherwise noted. To compensate for losses due to evaporation, deionized water was added daily to reestablish cultures to 600 mL.

The effect of the superficial gas velocity of the riser, U_{gr} , on the growth rate of *I. galbana* was studied in batch mode. Airlift vessels were sparged with different air flows: 0.5 vvm, 1.0 vvm, 2.0 vvm, 4.0 vvm and 6.25 vvm, and used a uniform sparger diameter of 1.6 mm. At the highest air flow, 6.25 vvm, a 7.5 cm diameter extender was needed to prevent media loss due to the increase in gas holdup, and therefore overall volume, within the cylinder. The extender was made of opaque PVC in order to keep the illuminated surface area the same, and had the same dimensions as the original airlift.

The effect of the sparger velocity, v , on growth rate was investigated by maintaining a uniform air flow (2.0 vvm) and using different diameter spargers (0.58 mm, 0.84 mm, 1.6 mm, 3.2 mm) with an open pipet, the luer lock attachment, and gauge 18 and 20 stainless steel needles, respectively.

To test the effects of bubble size on growth rate, cultures were grown using (1) a fine pore diffuser with smaller diameter pores, 3.8 cm x 1.2 cm, bubble size 0.5 to 2 mm, (2) a medium pore diffuser, 3.8 cm x 1.2 cm, bubble size 1 to 3 mm (A1, Aquatic Ecosystems), and (3) and a 3.2 mm diameter glass pipet (“open”), bubble size was not measured but observed to be much greater than the bubble size of the spargers. Bubble size was assumed to remain constant throughout the experiment. The maximum particle size specification, which represents the largest size particle that can pass through the diffuser, was 50 μm and 25 μm for the medium and fine pore diffusers as indicated by the manufacturer, respectively. The diffusers were attached to the glass pipets with 1.2 cm truncated syringe pieces, as seen in Figure 2.1(C). Air flow was maintained at 2.0 vvm. The gas diffusers were only used once per experiment, to avoid having used spargers whose pores might be clogged. Samples to measure cell densities were taken every two hours after the start of the experiment to closely monitor the effects of the diffusers.

Three replicates of each culture were monitored in each trial. Each experiment was performed twice. For statistical purposes, each replicate in each trial was considered to be an individual data point.

3. Results and Discussion

3.1. Effects of superficial gas velocity

The effect of air flow on the growth of *I. galbana* was examined over a period of two weeks. The final cell density, at the end of log-phase growth, for *I. galbana* is shown in Figure 3.1. The cell density increased linearly with each increase of air flow, up to 6.25 vvm, or 8.0 cfh². The maximum cell density was 56×10^6 cells mL⁻¹. The maximum specific net growth rate (μ_{\max}), 0.0288 h⁻¹, was achieved by the airlift reactors with the highest air flow rate within the first 48 hours, as indicated in Table 3.1. The first trial of the two replicates failed because of contamination of the cultures.

Table 3.1: Maximum specific net growth rate as affected by air flow and gas velocity.

Air Flow			Superficial gas velocity in riser, U_{gr} (mm s ⁻¹)	Maximum specific net growth rate, μ , (h ⁻¹)
(cfh)	(lpm)	(vvm)		
0.6	0.3	0.5	7.0	0.0175
1.2	0.6	1.0	14.0	0.0211
2.4	1.1	2.0	29.7	0.0232
5.0	2.4	4.0	58.2	0.0277
8.0	3.8	6.25	93.0	0.0288

Figure 3.1 depicts the cell densities of each of the cultures over the 120 hours, while Figures 3.2 and 3.3 present the growth rate over time. The μ_{\max} and the final cell density increased with increased superficial gas velocity. No negative effect on growth of *I. galbana* was observed at the highest superficial gas velocity. A p-value of 0.000006 was calculated using the ANOVA test with U_{gr} as the source of variance. A subsequent LSD test showed that each pair of experimental conditions had significance less than 0.05.

² Cubic feet per hour, a measurement of air flow.

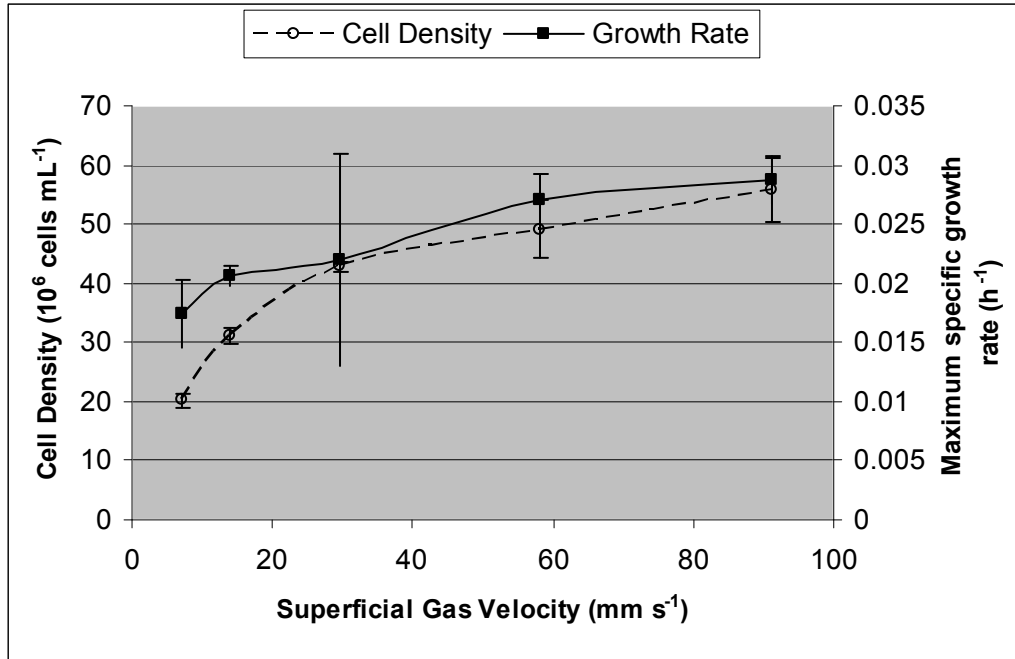


Figure 3.1: Effect of superficial gas velocity in the riser, U_{gr} , on the cell density of *I. galbana* at 120 hours. The increase in air flow corresponded to an increase from 7 mm s⁻¹ to 93 mm s⁻¹ in the velocity in the riser. Maximum growth rates are shown for each of the gas velocities. Error bars represent ± 1 standard deviation.

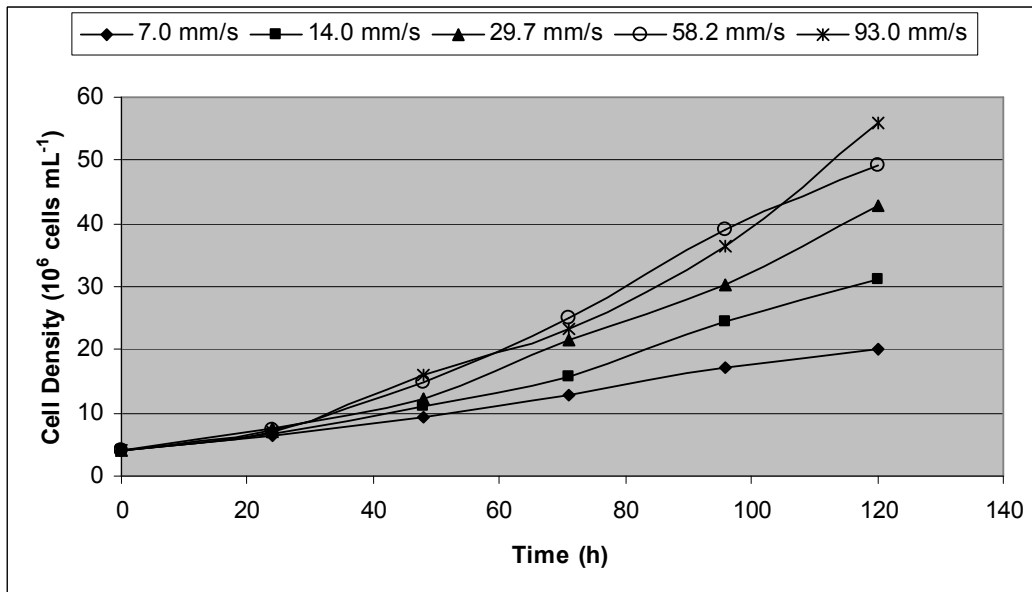


Figure 3.2: Growth curve of *I. galbana* grown in batch culture at different superficial gas velocities (7.0, 14.0, 29.7, 58.2, 93.0 mm s⁻¹) in a split-cylinder internal-loop airlift photobioreactor at 20°C.

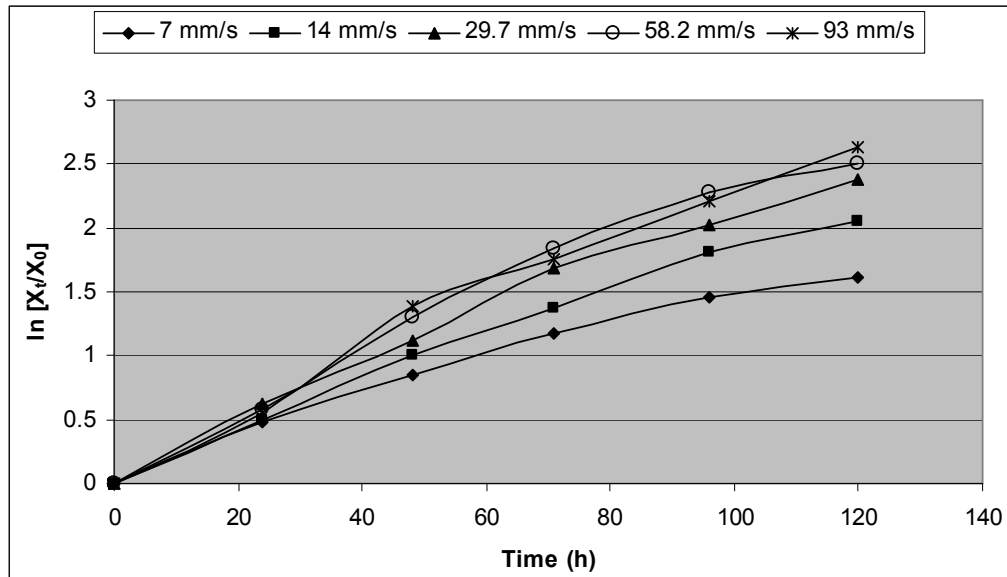


Figure 3.3: Growth rates of *I. galbana* cultured at different superficial gas velocities, 7-93 mm s⁻¹. The lag phase was almost non-existent, and the highest growth rates occurred within the first 48 hours.

For most microalgae species, increasing the superficial gas velocity, U_g , in an airlift or bubble photobioreactor will increase growth rates until a certain air flow, at which point further increases cause cell damage and decrease the growth rate (Suzuki, 1986). The data collected in this study suggest that for *I. galbana*, the point at which U_g is harmful rather than advantageous is higher than 6.25 vvm, or 93 mm s⁻¹. Unlike the results of Vega-Estrada (2005) for *H. pluvialis*, it can be concluded that *I. galbana* is not susceptible to the effects of increased superficial velocity.

Figure 3.4 shows that the relationship between U_{gr} and the mass transfer coefficient k_{La} was linear. The growth rates and final cell densities closely parallel the increase in the k_{La} . As a measure of the overall mass transfer of oxygen, k_{La} is an important criterion because it has been shown to be proportional to $k_{La}[CO_2]$ (Aitchison et al., 2007).

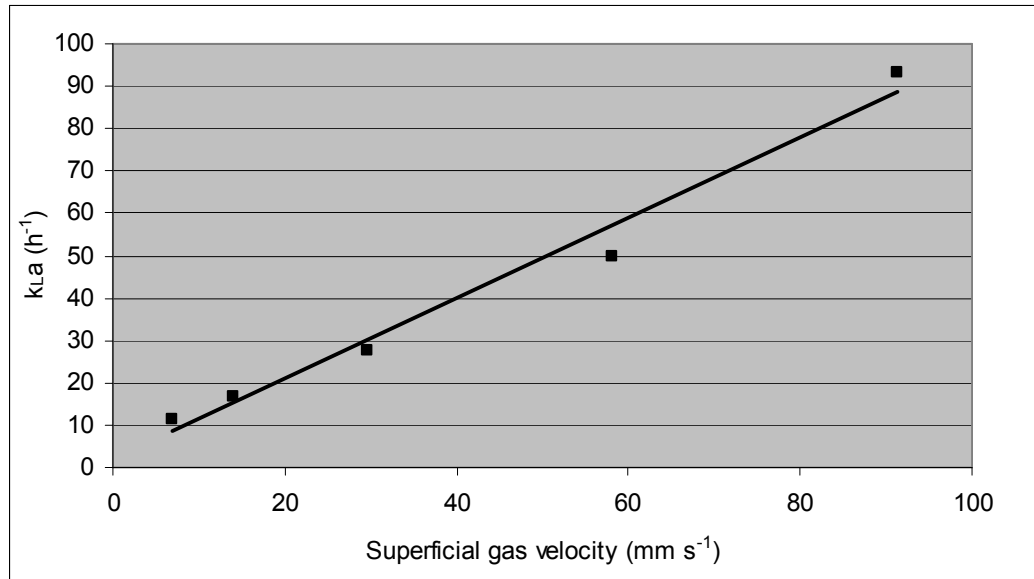


Figure 3.4: Mass transfer coefficient, $k_{L}a$, as a function of superficial gas velocity in the riser, U_{gr} . The diameter of the sparger was held constant at 1.6 mm. The linear regression line has the equation $k_{L}a = 0.95U_{gr} + 1.78$, with an R^2 of 0.98.

Microalgae such as *I. galbana* obtain inorganic carbon by fixing gaseous carbon dioxide. The values of the pH on day 5 of the experiments were 9.2 ± 0.2 . *I. galbana* has been shown to decrease growth rates at pH values above 9.0 (Kaplan, 1986). This does not invalidate the conclusions, but it may explain the limitation to exponential growth after 120 hours.

Two of the limiting factors in microalgae culture are access to light and access to gas exchange (Tredici, 1999). The data suggest that access to gas exchange might be more important than access to light at lower densities under conditions where CO_2 is not supplied in excess. If light were the limitation for these cultures, it could be expected that the cultures with the slower growth rates would remain in exponential phase the longest, because light would be able to penetrate further for longer. The data imply that because all cultures had access to the same light, the higher $k_{L}a[CO_2]$ values in the culture with the highest superficial gas velocity may have contributed to higher growth rates.

Merchuk et al. (2000) found a negative effect when using U_g values between 0.54 and 8.2 mm s⁻¹ for *Porphyridium*, while Suzuki et al. (1995) reported that U_g values greater than 17 mm s⁻¹ had a negative effect on *D. tertiolecta*. Sanchez-Miron et al. (2003) found that *Phaedactylum tricornutum* cells were susceptible to hydrodynamic stress when the velocity exceeded 10 mm s⁻¹. Barbosa (2003) used higher values for *D. tertiolecta* (76 mm s⁻¹) and *Chlamydomonas reinhardtii* (85 mm s⁻¹) and did not see negative results. Vega-Estrada (2005) used a similar split-cylinder device as used in the research reported here to test the effects of aeration, and found that *Haematococcus pluvalis* cells were sensitive for gas velocities greater than 12 mm s⁻¹.

The upper range of volumetric air flows (0.5 to 6.25 vvm) used in these trials was much higher than that of other researchers, who have experimented only up to 2.0 vvm. Given this body of work and particularly the current results of the present study, *I. galbana* (T-ISO) CCMP 1324 can be classified as a hardy species with respect to hydrodynamic stresses induced by the superficial gas velocity.

3.2. *Effects of sparger velocity*

Sparger velocities greater than 2.5 m s^{-1} were found to slightly reduce growth rates in *I. galbana* grown in batch cultures. For the four diameter spargers used (0.58 mm, 0.84 mm, 1.6 mm, 3.2 mm) values of the equivalent sparger velocity and Reynold's number, as calculated from Equation 2.4, are presented in Table 3.2.

Table 3.2: Experimental conditions for sparger velocity experiments.

<i>Group</i>	<i>Diameter sparger, d_i (mm)</i>	<i>Sparger velocity, v (m s^{-1})</i>	<i>Reynold's number at orifice</i>
I	3.20	2.48	23700
II	1.60	9.93	47400
III	0.84 (Gauge 18)	35.6	89800
IV	0.59 (Gauge 20)	73.4	129000

Cell densities in late-log phase growth at 120 hours are depicted in Figure 3.5. Growth rates for the same four conditions in their exponential phase are presented in Figure 3.6. Final pH values for all cylinders were 9.2 ± 0.2 on day 5, and salinity values were 31 ± 1 ppt.

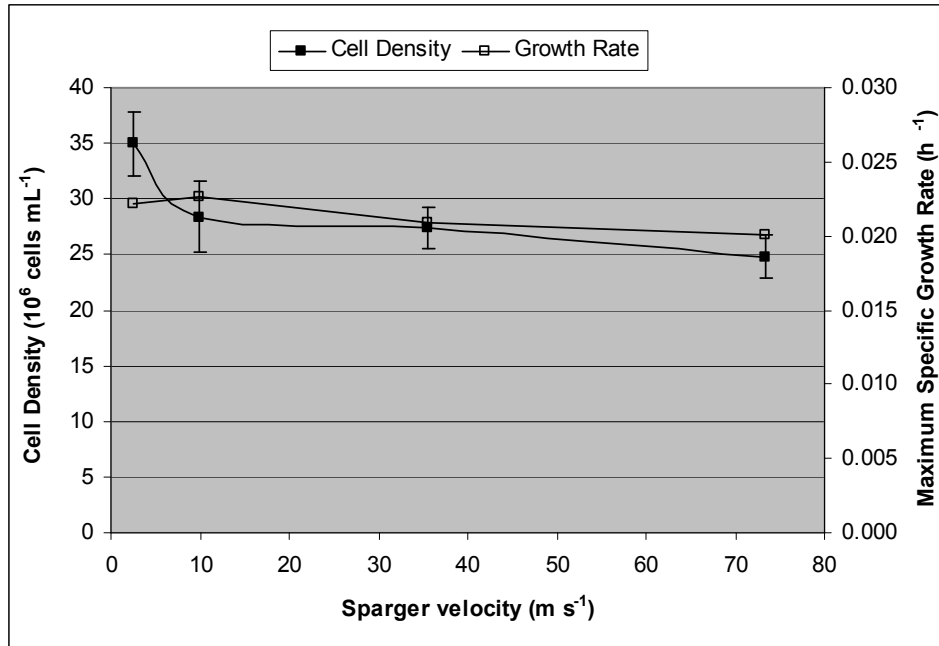


Figure 3.5: Effects of increased sparger velocity on the cell density of *I. galbana* at 120 hours. Sparger velocity was increased by decreasing the sparger diameter, including 3.2 mm, 1.6 mm, 0.84 mm and 0.59 mm. Air flow was held constant at 2.0 vvm. Error bars represent ± 1 standard deviation.

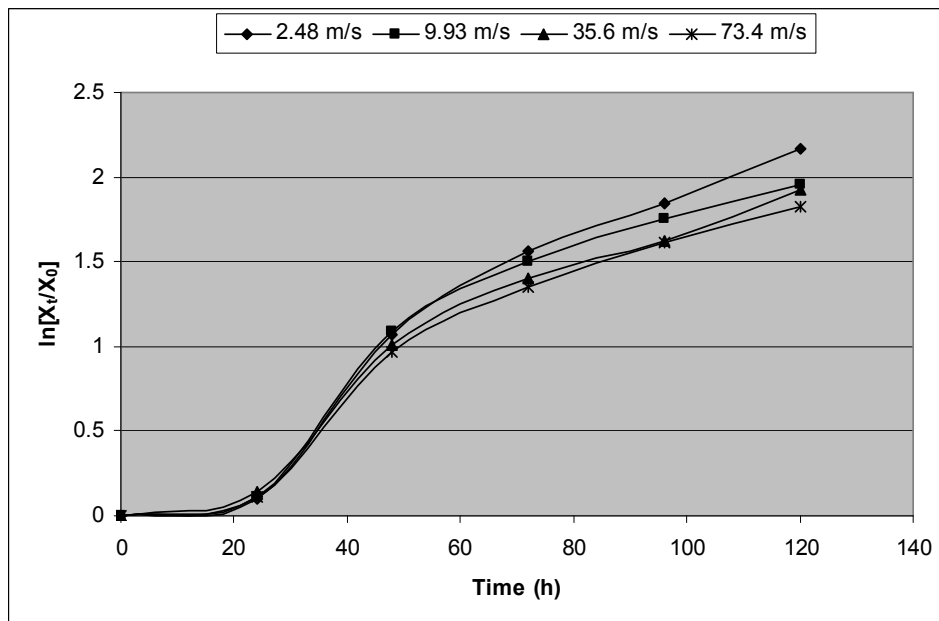


Figure 3.6: Growth rates of *I. galbana* cultivated at different sparger velocities (2.48, 9.93, 35.6, 73.4 m s⁻¹) for (a) Run 1 and (b) Run 2. The lowest velocity performed nominally better than higher velocities.

There was a clear trend showing that the 2.48 m s⁻¹ sparger velocity performed better than higher velocities. A single-factor ANOVA test using superficial gas velocity as the variable tested when analyzing the cell density, confirmed this. The test showed that there was a statistically significant difference between the results (p=0.00009). A subsequent post-hoc test resulted in statistically significant results as shown in Table 3.3. Significant results were reported between the 2.48 m s⁻¹ group and each of the other groups, and between the 9.93 m s⁻¹ group and the 73.4 m s⁻¹ group. It can be concluded that superficial gas velocity has a significant impact on the growth of *I. galbana*.

Table 3.3: Results (p-values) of an LSD post-hoc test on sparger velocity data. The group numbers correspond to the experimental conditions as described in Table 3.2. Significance (p<0.05) is reported between groups I and II, III and IV, and groups II and IV, as shown by the boldfaced type.

	<i>I</i>	<i>II</i>	<i>III</i>	<i>IV</i>
<i>I (3.20 mm)</i>	-	.000	.000	.000
<i>II (1.60 mm)</i>	.000	-	.507	.024
<i>III (0.844 mm)</i>	.000	.507	-	.094
<i>IV (0.586 mm)</i>	.000	.024	.094	-

Figure 3.7 shows that the k_{La} fluctuated between 20.6 and 28.0 for the sparger diameters, with the larger velocities having the highest k_{La} values. Higher k_{La} values should correspond to higher growth because more carbon dioxide is available to the cells, but in this case, the higher value corresponded to less growth. This indicates that the transfer of gas in the culture was not the cause for the results showing that the lowest sparger velocity airlifts performed the best. In the previous experiments, higher k_{La} values corresponded directly with higher growth rates, therefore the highest sparger velocities may have had an even greater detrimental effect than shown in these trials.

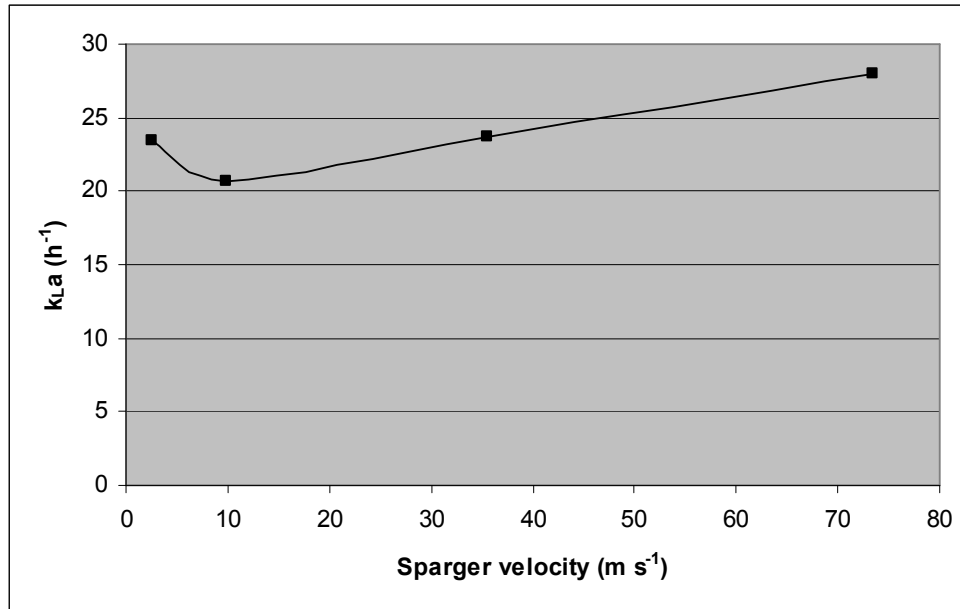


Figure 3.7: Mass transfer coefficient, k_{La} , for spargers ($n=1$) as a function of sparger velocity, as measured in seawater at 20°C. Air flow was held constant at 2.0 vvm, or U_{gr} equal to 29.7 mm s⁻¹.

The literature supports increased sparger velocities having a negative effect on cell growth. Shear stress at the sparger site due to formation and breakup of bubbles was first identified by Silva et al. (1987) as a possible cause of cell damage in *Dunaliella* (of unidentified strain). Silva et al. (1987) found, using Re numbers between 9.9×10^4 and 18.8×10^4 (which by the author's calculation corresponded to sparger velocities between 22.3 m s⁻¹ and 41.4 m s⁻¹) that cell productivity decreased by 80%. Later, Suzuki et al. (1995) experimented with sparger velocities between 13 and 125 m s⁻¹ on *Dunaliella tertiolecta*. He discovered that the death rate increased with an increased sparger velocity. The work of Barbosa (2003) investigated sparger velocities by increasing the number of spargers, rather than changing the diameter of the sparger. She found that sparger velocities of 66.3 m s⁻¹ (with Re calculated to be approximately 35,300³) contributed to the death of *H. pluvalis* cultures, while 7.4 m s⁻¹ did not have a death rate, and concluded that there was likely a critical sparger velocity for each

³ $\rho = 1000 \text{ kg m}^{-3}$, $\eta = 0.001 \text{ Pa s}$

species. It should be noted that Barbosa and Suzuki et al. were interested only in death rates and did not extend the experiments to see if there would be lower growth rates for cultures that survived higher velocities. Garcia-Camacho et al. (2000) did not find a negative effect up to 24 m s^{-1} (Re not available) for *P. tricornutum*, but found lower growth rates at 47.8 m s^{-1} , while Vega-Estrada reports decreased growth for *H. pluvalis* for sparger velocity greater than 22.8 m s^{-1} (Re approximately 97,300).

The position of the sparger may have an effect on the flow dynamics created in the airlift reactor. Chisti (1987) found from visualization studies that the position of the sparger had a large impact on bubble coalescence, which was often neglected in previous studies (Petersen, 2001). They found that if the sparger is placed at the entrance of the riser, the downcomer stream entering the riser would shift the gas bubble stream from the sparger, creating a channel along the opposite wall. This had the effect of increasing bubble coalescence and bubble size, and therefore decreasing the $k_L a$. When the sparger was placed just inside the riser, the downcomer flow joined the riser under the sparger for better gas distribution results. Further studies involving gas sparger location are needed to understand how the different variables affecting flow dynamics relate to cell growth in microalgae.

The results show that reduced growth rates for *I. galbana* (T-ISO) CCMP 1324 may be caused by increased sparger velocity, confirming the analysis by Barbosa (2003) that sparger site may be an important contributor to aeration-induced hydrodynamic stress. The range of sparger velocities (2.5 to 73.4 m s^{-1}) used in these trials was comparable to that of other researchers, yet instead of inducing a death rate, *I. galbana* maintained a final cell density at the highest sparger velocity ($v = 73.4 \text{ m s}^{-1}$) that remained at over 70% of the cell density of the lowest sparger velocity ($v = 2.5 \text{ m s}^{-1}$). *I. galbana* may be a hardier species in this regard than *Dunaliella*, *H. pluvalis*

and others. However, the data suggest that sparger velocities greater than 2.5 m s^{-1} have a negative effect on the growth of *I. galbana*.

3.3. Effect of gas diffusers

Diffuser pore size had a significant impact on the growth of *I. galbana*, as depicted in Figure 3.8. For the first 24 hours, the fine pore and medium pore diffusers in two trials displayed severe negative growth as compared to the open pipet. For the fine pore diffuser, the largest negative growth was 0.12 h^{-1} , and for the medium pore diffuser the largest negative growth was 0.11 h^{-1} . In the first trial, the diffuser cultures began to experience positive growth after 8 hours, while in the second trial, positive growth occurred after 24 hours. There are less data points in the first trials because after 24 hours it was assumed that the culture was no longer viable, and measurements were not taken. The statistics were calculated separately for each trial. In both trials, a foam layer was visually observed in both the fine pore and medium pore diffusers in the first 24 hours but not in the open pipet reactor. The foam layer diminished over the five day period.

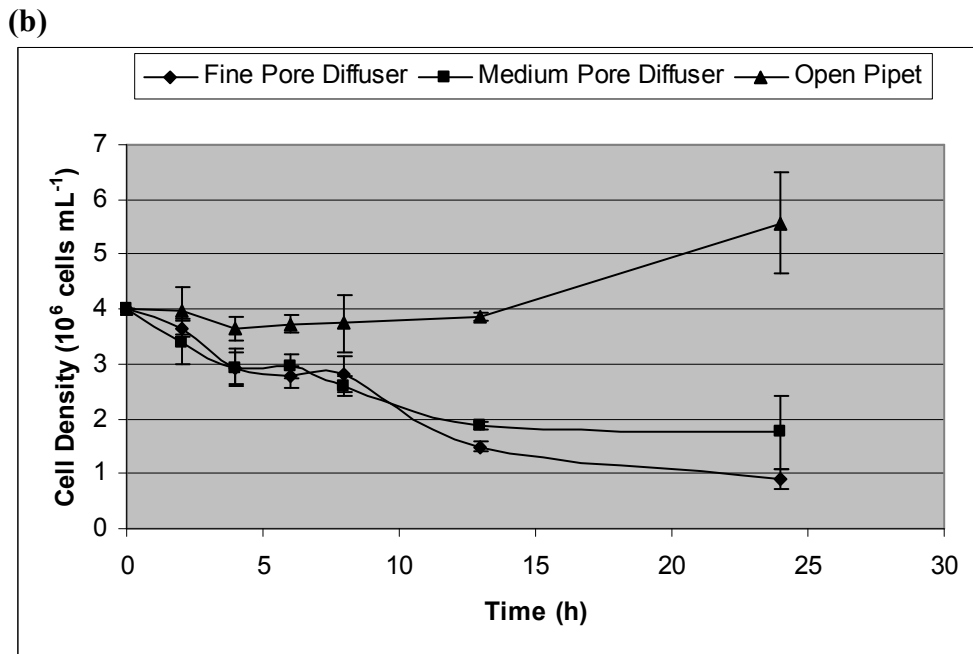
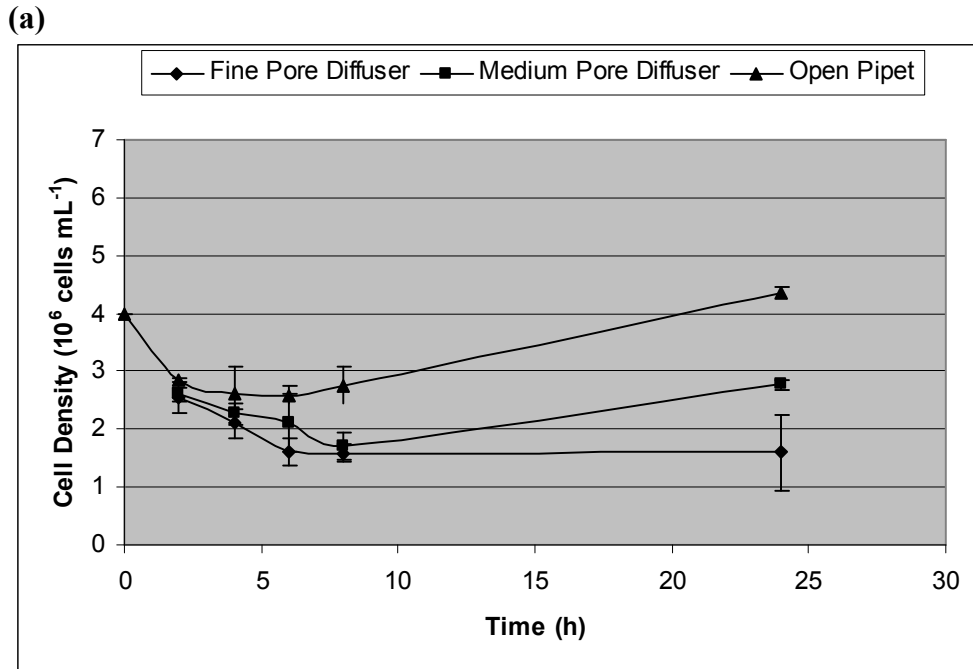


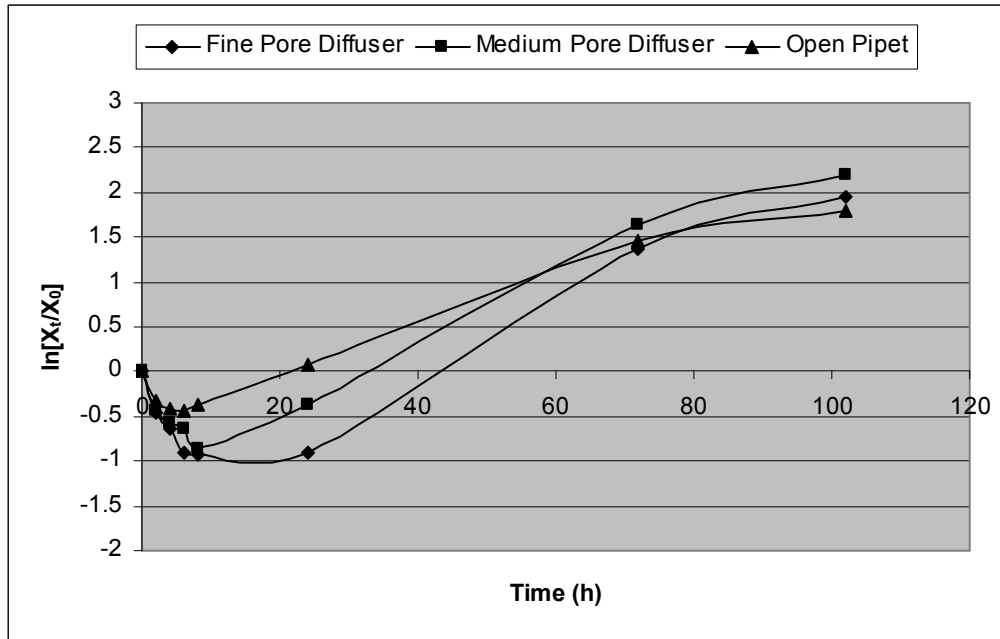
Figure 3.8: Effects of three different sizes of bubbles on *I. galbana* over the first 24-hour period in a bench-scale split-cell photobioreactor. Cultures showed a more pronounced death rate in (b), Run 2, than (a), Run 1. In both cases, the cultures with diffusers had a negative specific growth rate for the first 24 hours.

As seen in Figure 3.9, although the death rate was much greater than the growth rate during the lag phase, the growth rate outpaced the death rate for both experiments.

Due to the fact that the second experiment had more data points than the first, it is possible to see in Figure 3.9(b) that the growth rates immediately after the lag phase, between 24 and 48 hours, were approximately equal (0.035 h^{-1} , 0.036 h^{-1} and 0.037 h^{-1} for fine pore, medium pore and open pipet, respectively). After 48 hours, the growth of the medium pore and fine pore diffusers was higher than the growth of the open pipet cultures (Figure 3.9). At 24 hours, an ANOVA test on the combined data sets (Run 1 and Run 2) showed significance ($p < 0.0001$), and an LSD test confirmed significance between each of the conditions.

In the end, the final cell densities of the cultures were highest in the medium pore diffusers, followed by the fine pore, and then the open pipets (Figures 3.9 and 3.10). In the first experimental trial, one of the fine pore diffuser replicates ended at only $14 \times 10^6 \text{ cell mL}^{-1}$, contributing to the high standard deviation, while the two other replicates had a final cell density higher than the medium pore cultures (34 and $38 \times 10^6 \text{ cell mL}^{-1}$). An ANOVA test comparing the final cell density of three different sparger types at 120 hours using the second set of experimental results showed statistical significance, with the p-value equal to 0.004. An LSD post-hoc test showed significance in cell density between the open pipet and the medium pore diffuser type (significance level = 0.004) and between the diffuser types (significance level = 0.002), but not between the fine pore diffuser and the open pipet (significance level = 0.620). The first set of experimental results, at 100 hours, did not show significant differences using an ANOVA test.

(a)



(b)

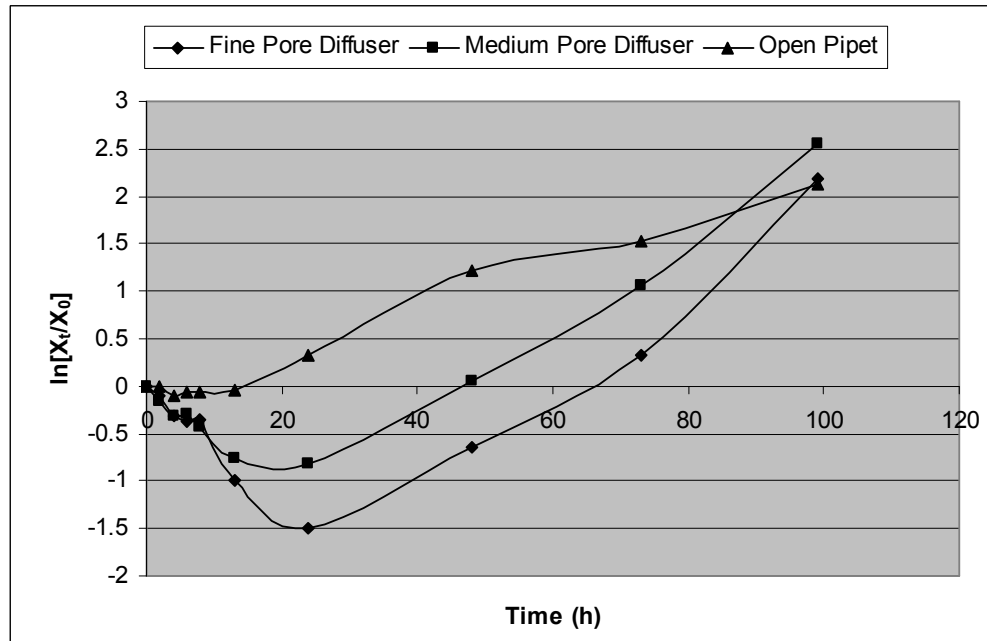


Figure 3.9: Growth rates of *I. galbana* cultured with different diffuser types presented for two trials over 100 hours, (a) and (b). Growth was negative for the first 24 hours for both of the diffusers. Between 24 and 48 hours, the growth rate of three conditions was approximately equal. After 48 hours, the diffusers outpaced the open pipet. Air flow was constant at 2.0 vvm, or 29.7 mm s⁻¹.

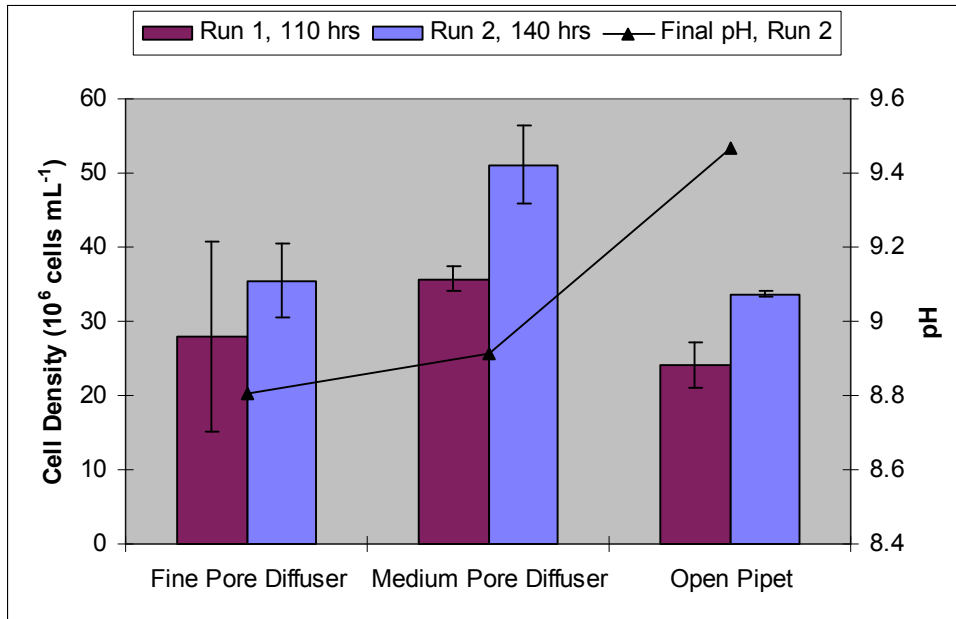


Figure 3.10: Final cell densities and pH for each of the diffuser configurations. Although the open pipet was the most successful over the first 24 hours, the higher $k_L a$'s of the fine pore and medium pore diffusers allowed for better gas exchange and faster growth rates in exponential phase.

The $k_L a$ values, shown in Figure 3.11, were 23.4, 258 and 573, for the open pipet, medium pore diffuser and fine pore diffuser, respectively, as calculated using Equation 2.8. In these experiments the benefits of increased gas exchange created an environment for a much higher growth rate for the cultures with diffusers that extended a longer period of time. The maximum overall growth rates, occurring between 24 and 48 hours, suggest that it was primarily the lag phase that was affected by the small bubbles and the presence of the diffusers. This is most likely because the overall death rate was increased, and there was little growth in the lag phase.

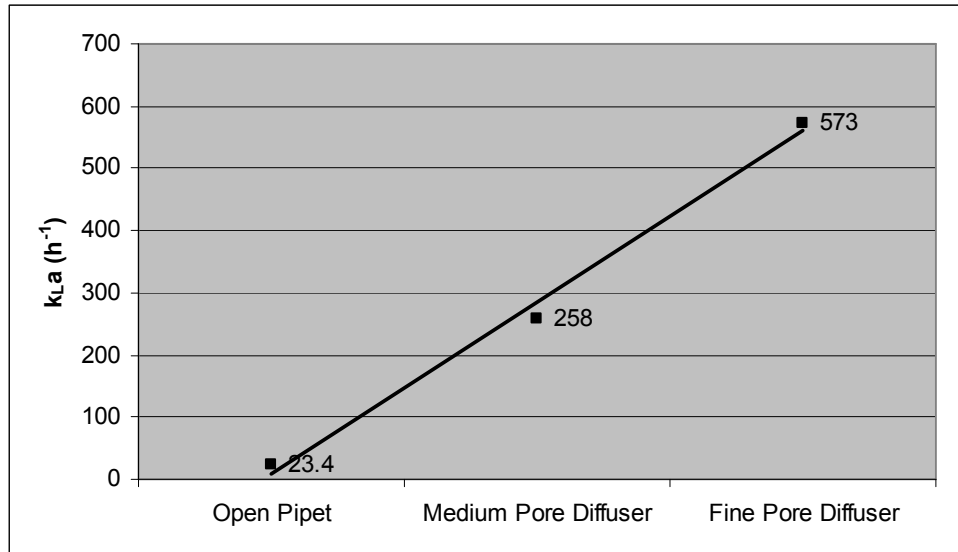


Figure 3.11: Mass transfer coefficients, $k_{L,a}$, measured for different types of diffusers. The superficial gas velocity was held constant at 29.7 mm s^{-1} . Bubble sizes for the medium pore diffuser were between 1.0 and 3.0 mm, while bubble sizes for the fine pore diffuser were between 0.5 and 2.0 mm.

It is possible that the change in bubble size contributed to the increased death rate. Aeration of suspended cells with excessively small bubbles has been associated with cell ‘wash out’ into a stable foam layer by a froth flotation mechanism in large scale reactors. The mechanism of foam formation in the bench-scale reactors is similar to that used in foam fractionators, except that there cannot be washout in a closed reactor. Since the foam is associated with cell destruction, and there was more foam present in the airlift reactors with diffusers, the small bubble size in the diffusers can be correlated with cell damage. The visual observation that foam was reduced significantly in after 24 hours matches well with the data showing exponential cell growth in the same period.

There is sufficient experimental evidence that bubble rupture at the surface, leading to foam formation, can be a major cause of cell death (Wang et al., 1994). Garcia-Camacho et al. (2001) reported that the break-up of small bubbles on the liquid surface was the cause of cell damage in the microalgae *P. tricornutum* when U_g is between 0.01 and 0.05 m s^{-1} . Microscopic visualization studies have confirmed cell

attachment to bubbles (Petersen, 2001). In the results reported in the present study, bubble bursting at the surface is a possible cause, but does not explain why after 24 hours the cultures stabilized and were able to grow faster than the open pipet (as seen by comparing Figures 3.8 and 3.9).

Larger bubbles (such as those associated with taller columns) have been found to produce more stable foams than small bubbles (Molina Grima et al., 1997). This, however, contradicts the need for high gas transfer rates that are achieved by creating smaller bubbles. Especially in serpentine tubular reactors, where the culture is typically only exposed to gas exchange once every three to five minutes, maximum gas transfer rates are necessary to avoid oxygen accumulation and high pH associated with inadequate CO₂. In the bench-scale airlift reactors, higher k_La 's were shown in this report to correlate to higher cell densities. Therefore there is a tradeoff between the detrimental effects of small bubbles (through foam formation or surface bursting) versus the beneficial effects of higher gas transfer.

The final cell densities are shown in Figure 3.10. The medium pore diffuser cultures, although they had a k_La value that was only 45% of the fine pore diffuser airlift, succeeded in outperforming the other cultures by the end of the second experimental trial. It is possible that the smaller bubble size in the fine pore diffuser, through foam formation and bubble bursting at the surface, inhibited the growth rate in comparison to the medium pore diffuser. Or, because the effects were so severe in the first 24 hours, the fine pore diffuser was never able to catch up to the final cell density of the medium diffuser. Given enough time, the fine pore diffuser might have reached the same cell density as the medium pore diffuser, but only because the medium pore diffuser would have entered stationary phase. The open pipet cultures, with the largest bubble size, had final densities less than that of the medium pore diffuser, yet had a higher growth rate in the first 24 hours. Although the larger bubble size likely had a

smaller negative effect on growth, it also had a much lower k_{La} , which limited its overall growth potential.

Lastly, it remains to be considered whether the physical presence of the diffuser (1.25 cm in width) may have induced a mechanical stress due to direct contact with the cells. The entire area of the riser was only 6.75 cm², while the cross-sectional area of the diffuser itself was 2.25 cm². If researchers have found that the presence of a baffle may induce stress (Barbosa, 2003), it is possible that this may also explain partially the death rate in the diffuser experiments. It does not explain, however, why the cultures were revived after 24 hours.

Although experiments exactly like this one have not been performed for a direct comparison with other species, it seems that the growth rate of *I. galbana* (T-ISO) was very sensitive to bubble size. The exponential death rate within the first 24 hours for the two types of diffusers indicates that the diffusers (either the bubble bursting at the surface or direct contact with the cells) played a role in inducing shear stress. The exact mechanisms that caused the reduced overall growth rate remain unclear, but it is recommended that the tradeoff between lower gas transfer available with large bubbles and the possibility of cell damage due to small bubbles be considered when designing an air inlet.

The results provided by this experiment showed that the air flow alone, in the form of superficial gas velocity and sparger velocity, cannot predict the level of hydrodynamic stress experienced by the culture, and that other sources of stress should be identified.

3.4. Implications for airlift-driven tubular photobioreactors

Researchers have shown that the diameter of the tubes in tubular reactors greatly influences the amount of light available (Hu and Richmond, 1994; Molina-Grima et al., 2001), yet large-scale microalgae production requires large-volume reactors that are most easily achieved with larger tube diameters. The circulation of larger volumes of algae requires more air in an airlift-driven system. In larger scale air-driven systems, an increase in pneumatic power is needed to support sufficient mixing levels. Short-circuiting may become a problem, and additional power may be needed to maintain effective mixing, thereby causing higher shear conditions.

The results of this work have shown *I. galbana* to be sensitive to bubble size, but there is not enough information to discern whether or not diffusers would be harmful to this microalgae at a larger scale. Smaller bubbles, especially from air diffusers, have been shown here to induce stress on *I. galbana*. The causes of the hydrodynamic stresses due to small bubbles are not completely understood, but can be postulated to originate from two sources: first, from the change in surface tension as the bubble reaches the liquid-air interface, and second, from the frictional forces associated with contact with the walls of the diffuser. At a larger scale, contact with the diffuser would be significantly less.

At the laboratory scale, several authors have concluded that the main cause for cell damage was the bubble bursting at the liquid surface (Suzuki et al., 1995; Chisti, 1999; Garcia-Camacho et al., 2001). For larger volume reactors, reactor designers rarely choose to use air diffusers to drive the airlift, and instead choose to use gas spargers which can provide the large volume of air using few parts while avoiding the risk of clogging. Tubular photobioreactor researchers have noted that smaller bubbles are more efficient at gas transfer (Babcock, 2002) and therefore desirable, yet the experimental results shown in this paper suggest that using solely fine pore diffusers to

provide air for a large volume reactor may reduce growth rates for *I. galbana*. A combination of larger diameter gas spargers and diffusers may deliver both high volumes of air to induce mixing and small bubbles to increase gas exchange.

It may also be inferred from the data that the initial lag phase is the most critical period, because in this period the death rate is greater than the growth rate. Research has shown that continuous systems, as opposed to batch systems, offer high productivity and stability when the dilution rate is maintained lower than the growth rate of the species. Continuous systems, once initiated, do not have a lag phase that would be affected. In this regard, bubble size may not play a significant role in a scaled-up reactor.

At a larger height scale, some of the small bubbles formed by the diffuser would coalesce, reducing the overall gas transfer coefficient for the reactor and reducing the likelihood of cell death due to bubble bursting at the surface. On the other hand, a tall column (often upwards of 3 m) would have a significant pressure difference between the bottom of the column and the surface, which may lead to hydrodynamic stresses on the microalgae due to the rapid change in pressure as the cells travel from the bottom to the top of the reactor or column. Few researchers have reported on this topic. Camacho et al. (2000) indicated a rise in death rate associated with increased culture height for *P. tricornutum*, in opposition to the findings of Suzuki et al. (1995) for *D. tertiolecta*. The present study did not address the question of whether bubble rising has a positive or negative effect on the growth rate of *I. galbana*. Further work regarding the effects of the height of the column would clarify the relationship between the superficial gas velocity and the column height for *I. galbana*.

The role of aeration in the scale-up of algal photobioreactors is still poorly understood. Few researchers have investigated the effects of gas velocity in production- or pilot-scale reactors, with the more recent notable exceptions of

Camacho et al. (2001) and Barbosa (2003). Barbosa used a 69 L pilot plant to research the effects of aeration on *D. tertiolecta* and found that cell damage was present at velocities lower than the superficial gas velocities found to be harmful in lab scale experiments. She attributed this to a much higher sparger velocity. In general, it seems that because the energy due to aeration is distributed over a larger volume, scale up of air flows and addition of diffusers is less likely to cause damage in large scale reactors than bench-scale reactors. At the sparger site, on the other hand, the energy is not being distributed over a larger area or volume unless it is designed that way. There is more potential for a stress event to happen due to sparger velocities.

It is suggested that for photobioreactors using either an airlift or bubble configuration, gas flow be increased as much as economically possible (to 100 mm s^{-1} or higher) to maximize gas exchange and to increase the frequency of access to light for each individual *I. galbana* algae cell. Gas flow may be also distributed over a manifold of spargers to reduce the damaging effects of excessive sparger velocity. If oxygen or carbon dioxide transfer is a design limitation in a tubular photobioreactor system, the use of additional diffusers during the exponential growth phase of the culture may provide a method to increase gas transfer.

The conditions tested at the laboratory scale in this work identify important variables for consideration in a typical large-scale serpentine tubular reactor. Using this, and the information presented in Table 3.4 (see Design Example that follows), the growth of *I. galbana* is most likely to be affected by excessive sparger velocities. It is quite plausible that when scaling up aeration to meet circulation requirements there would be a non-linear response; however, the data suggests that *I. galbana* would not be greatly affected by the volume of air (vvm) or gas velocities (U_g) typical of large-scale reactors, indicating its suitability for use in photobioreactors.

3.5. Design Example

Table 3.4 describes the air flow requirements to circulate a 100 m serpentine tubular bioreactor at the recommended 35 cm s^{-1} velocity (Richmond, 1993; Tredici, 1999; Acien-Fernandez et al., 2001; Chisti, 2007) using an 8 ft airlift column and approximately 12 inches of head loss in the system. Figure 3.12 depicts the model system used. Calculation of approximate head loss is presented in Appendix C.

Table 3.4 Typical values needed for 0.35 m s^{-1} liquid velocity in airlift-driven tubular photobioreactors. Air flow rates adapted from data by Timmons et al. (2002). Airlift assumed to be 2.4 m (8 ft) in height with 30.5 cm (12 in) of overall head loss, including elevation change.

Diameter Airlift (in)	Diameter Airlift (cm)	Liquid Flow Rate (lpm)	Air Flow Rate (lpm)	Air Flow (vvm)	U_g (mm s^{-1})	v ($n = 1$), $d_i = 3.2$ mm (m s^{-1})	v ($n = 1$), $d_i = 6.4$ mm (m s^{-1})
1	2.5	10.6	3.1	2.49	101	6.5	1.6
2	5.0	42.6	12.7	2.58	105	26.8	6.7
3	7.6	95.9	30.2	2.72	111	63.6	15.9
8	20.3	682.0	316.0	4.01	163	667.0	167.0

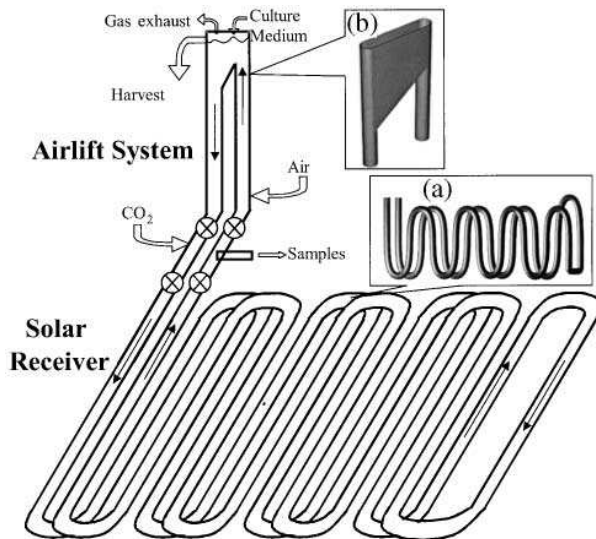


Figure 3.12: Typical serpentine tubular reactor, as designed by Acien-Fernandez et al. (2001)

Given flow rate, head loss, airlift height and airlift pipe diameter, it is possible to calculate the required air flow needed to circulate the culture at a certain velocity

(Timmons and Ebeling, 2007). As shown in the table, the air flow described as vvm is relatively constant, while the sparger velocities increase dramatically with increased pipe diameters. While the volume of air required in larger volume reactors is increasing, the reactor is also increasing according to the square of the radius, thereby reducing the overall impact on the vvm. The sparger velocity, on the other hand, increases proportional to flow of air. The difference between a 3.2 mm air inlet and a 6.4 mm air inlet is substantial, especially for larger diameter tubes. Superficial gas velocities in the described hypothetical tubular bioreactor are higher than those used in this study (8 - 93 mm s⁻¹), but up to 3 in airlifts are within an order of magnitude. The former range of gas velocities has been inferred to have no effect on *I. galbana*.

Engineers of airlift-driven tubular bioreactors have the choice between two general designs: serpentine reactors and manifold reactors. Serpentine reactors use a single path length, and therefore usually require a smaller overall flow rate to achieve sufficient liquid velocities, and therefore mixing, for culture growth. Longer path lengths come with other disadvantages, specifically the build-up of oxygen and carbon dioxide gradients.

For manifold-style reactors such as those designed by Richmond (1993), the flow rate, and therefore the air flow, must increase proportionally to the number of parallel tubes. For species that have been shown to be sensitive to aeration, such as *Haematococcus sp.*, a major limitation to the scale up of manifold reactors is the aeration. Near horizontal tubular (NHTR) reactors, pioneered by Tredici (1999), use the advantages of manifold reactors to accommodate larger volumes while distributing the aeration requirements across the tubes. Babcock et al. (2003) built a near-horizontal tubular reactor (NHTR) that operated with a U_g less than 40 mm s⁻¹.

The data shown within this paper clearly indicate that for *I. galbana*, excessive shear stress due to superficial gas velocity is not a major engineering concern.

However, proper engineering of the spargers would distribute high air flows between many spargers, thereby reducing the sparger velocity and mitigating possible negative effects on growth rate. If a 7.6 cm diameter airlift reactor vessel was being designed, for instance, it is recommended for *I. galbana* to use at least a 6.4 mm diameter air sparger, or to divide the air flow amongst a number of smaller diameter air spargers. This would minimize the shear stress induced by the air flow at the sparger entrance while also providing gas transfer. It is also suggested that multiple spargers be used to lessen the turbulent force of the air. Given that culture collapse is likely for circulation velocities less than 35 cm s^{-1} because of lack of gas exchange and access to light, maintaining sufficient flow without damaging cells is a design priority for tubular reactors.

4. Conclusion

The effects of superficial gas velocity and sparger velocity on the growth of *I. galbana* (T-ISO) were investigated using 0.6 L split-cell internal airlift bioreactors under batch culture conditions. In addition, the effect of smaller sized bubbles on growth rate were examined using two different styles of diffusers while holding the overall air flow rate constant. For each of the aeration-related variables investigated, more work needs to be done to explain the relationship between bench-scale and production-scale systems, in order to better understand the process of scaling laboratory data to production-scale reactor design for different microalgal strains.

Based on these experiments, it can be concluded that:

- a. Increased air flow, up to 93 mm s^{-1} or 6.25 vvm, was positively correlated with increased growth when other variables were held constant.
- b. *I. galbana* is resilient in its tolerance to high superficial gas velocities and is a hardy species with respect to hydrodynamic stress.
- c. Increased sparger velocity greater than 2.5 m s^{-1} had a negative effect on growth rate of *I. galbana*.
- d. Superficial gas velocity and sparger velocity were not the only mechanisms responsible for hydrodynamic stress on *I. galbana*.
- e. Bubble size can negatively affect the growth rate of *I. galbana*.
- f. The presence of diffusers had a negative effect on the growth rate that was especially evident in the lag phase.

APPENDIX A

The length scale of microeddies, λ , may be estimated as follows (Kawase and Moo-Young, 1990):

$$\lambda = \left(\frac{\eta}{\rho} \right)^{\frac{3}{4}} \xi^{-\frac{1}{4}} \quad \text{Eq. A-1}$$

where η is the dynamic viscosity, ρ is the density of the fluid and ξ is the energy dissipation per mass. For tubular bioreactor applications, the specific energy dissipation in a tube depends on the pressure drop (Acien-Fernandez et al, 2001):

$$\xi = \frac{2C_f U_L^3}{\phi} \quad \text{Eq. A-2}$$

where U_L is the liquid velocity in the tubes, ϕ is the inner diameter of the tube and C_f is the Fanning friction factor, which is calculated as:

$$C_f = 0.0791 * \text{Re}^{-0.25} \quad \text{Eq. A-3}$$

where Re is the Reynold's number. The Reynold's number is defined as:

$$\text{Re} = \frac{\rho U_L \phi}{\eta} \quad \text{Eq. A-4}$$

These equations were solved using a liquid velocity of 50 cm s^{-1} , tube diameter 0.0508 m , η of 0.001 Pa s , and ρ of 1000 kg m^{-3} .

APPENDIX B

The composition of the f/2 media is as follows (Guillard and Ryther, 1962):

<i>Component</i>	<i>Stock Solution</i>	<i>Quantity</i>	<i>Molar Concentration</i>
NaNO ₃	75 g/L dH ₂ O	1 mL	8.82 x 10 ⁻⁴ M
NaH ₂ PO ₄ H ₂ O	5 g/L dH ₂ O	1 mL	3.62 x 10 ⁻⁵ M
Na ₂ SiO ₃ 9H ₂ O	30 g/L dH ₂ O	1 mL	1.06 x 10 ⁻⁴ M
Trace Metal solution	(see recipe below)	1 mL	

Trace Metal Solution:

<i>Component</i>	<i>Primary Stock Solution</i>	<i>Quantity</i>	<i>Molar Concentration in Final Medium</i>
FeCl ₃ 6H ₂ O	---	3.15 g	1.17 x 10 ⁻⁵ M
Na ₂ EDTA 2H ₂ O	---	4.36 g	1.17 x 10 ⁻⁵ M
CuSO ₄ 5H ₂ O	9.8 g/L dH ₂ O	1 mL	3.93 x 10 ⁻⁸ M
Na ₂ MoO ₄ 2H ₂ O	6.3 g/L dH ₂ O	1 mL	2.60 x 10 ⁻⁸ M
ZnSO ₄ 7H ₂ O	22.0 g/L dH ₂ O	1 mL	7.65 x 10 ⁻⁸ M
CoCl ₂ 6H ₂ O	10.0 g/L dH ₂ O	1 mL	4.20 x 10 ⁻⁸ M
MnCl ₂ 4H ₂ O	180.0 g/L dH ₂ O	1 mL	9.10 x 10 ⁻⁷ M

APPENDIX C

Calculation of head loss for a serpentine tubular photobioreactor was estimated as follows. It was assumed that the reactor was made of Schedule 40 PVC of pipe length, l , of 100 m, pipe diameter, ϕ , of 0.0508 m (0.166 ft) with 15 180° turns. The tube velocity, U_L , was chosen to be 0.35 m s⁻¹ (1.15 ft s⁻¹). The dynamic head was calculated as:

$$\frac{U_L^2}{2g} = \frac{(0.35 \text{ m/s})^2}{2 * 9.81 \text{ m/s}^2} = 0.00625 \text{ m}$$

The frictional head losses were estimated using the Darcy-Weisbach equation,

$$\Delta h = f * \left(\frac{l}{\phi} \right) \frac{U_L^2}{2g} \quad \text{Eq. A-5}$$

where Δh is the head loss due to friction. Using a frictional coefficient, f , of 0.019 for 0.0508m hydraulic diameter PVC, Δh is calculated to be 0.235 m (9.24 in).

The head loss due to dynamic losses incurred in the turns was calculated using the resistance coefficient, K . A 0.0508 m close-return bend has K value of 0.95. The dynamic head losses were estimated using:

$$\Delta h_d = K * \frac{U_L^2}{2g} \quad \text{Eq. A-6}$$

Using a dynamic head of 0.00625 m, as calculated above, Δh_d is 0.0059 m per bend. For 15 bends, this would yield a total Δh_d of 0.089 m (3.51 in). The total head loss was therefore estimated as:

$$\Delta h_{total} = \Delta h + \Delta h_d$$

or approximately 0.324 m (12.75 in).

REFERENCES

- Acien-Fernandez, F.G., Garcia-Camacho, F., Sanchez-Perez, J.A., Fernandez-Sevilla, J.M. & Molina-Grima, E. (1997). A model for light distribution and average solar irradiance inside outdoor tubular photobioreactors for microalgal culture. *Biotechnology and Bioengineering*, 55, 5, 701-715.
- Acien-Fernandez, F.G., Fernandez Sevilla, J.M., Sanchez-Perez, J.A., Molina-Grima, E., & Chisti, Y. (2001). Airlift-driven external-loop tubular photobioreactors for outdoor production of microalgae: assessment of design and performance. *Chemical Engineering Science*, 56, 2721-2732.
- Aitchison, T.F., Timmons, M.B., Bisogni, J.J., Piedrahita, R.H., & Vinci, B.J. (2007). Use of oxygen gas transfer coefficients to predict carbon dioxide removal. *International Journal of Recirculating Aquaculture*, 8, 21-42.
- Arathoon, W.R., & Birch J.R. (1986). Large-scale cell culture in biotechnology. *Science*, 232, 1390-1395.
- ASCE. (1992). Measurement of Oxygen Transfer in Clean Water, ANSI/ASCE Standard 2-91. 2nd edn. American Society of Civil Engineers, New York, 41 pp.
- Babcock, R.W., Malda, J., & Radway, J.C. (2002). Hydrodynamics and mass transfer in a tubular airlift photobioreactor. *Journal of Applied Phycology*, 14, 169-184.
- Barbosa, M.J., & Wijffels, R.H. (2004). Overcoming shear stress of microalgae cultures in sparged photobioreactors. *Biotechnology and Bioengineering*, 85, 78-85.
- Barbosa, M.J. (2003). Microalgal photobioreactors: scale up and optimization. Phd Thesis for Wageningen University.
- Barbosa, M.J. (2003). Hydrodynamic stress and lethal events in sparged microalgae cultures. *Biotechnology and Bioengineering*, 83, 112-120.

- Benemann, J.R. (1992). Microalgae aquaculture feeds. *Journal of Applied Phycology*, 4(3), 233-245.
- Borowitzka, M.A. (1996). Closed algal photobioreactors: Design considerations for large-scale systems. *Journal of Marine Biotechnology*, 4, 185-191.
- Brindley-Alias, C., Garcia-Malea Lopez, M.C., Acien-Fernandez, F.G, Fernandez-Sevilla, J.M., Garcia-Sanchez, J.L., & Molina-Grima, E. (2004). Influence of power supply in the feasibility of *Phaedactylum tricornutum* cultures. *Biotechnology and Bioengineering*, 87, 723-733.
- Bronnenmeier, R., & Markl, H. (1982). Hydrodynamic stress capacity of microorganisms. *Biotechnology and Bioengineering*, 24, 553-578.
- Burgess, J.G., Iwamoto, K., Miura, Y., Takano, H., & Matsunaga, T. (1993). An optical fibre photobioreactor for enhanced production of the marine unicellular alga *Isochrysis aff. galbana* T-Iso (UTEX LB 2307) rich in docosahexaenoic acid. *Applied Microbiology and Biotechnology*, 39, 456-459.
- Burlew, J.S. (ed.). 1953. Algal Culture, From Laboratory to Pilot Plant. Publ. No. 600. Carnegie Institution of Washington, Washington, DC.
- Chisti Y. (1989). Airlift bioreactors. Elsevier.
- Chisti, Y. (1995). Relationship between riser and downcomer gas hold-up in internal loop airlift reactors with gas-liquid separators. *The Chemical Engineering Journal*, 57, B7-B13.
- Chisti Y. (1999). Shear sensitivity. In: Flickinger M.C., Drew S.W., eds. *Encyclopedia of Bioprocess Technology: Fermentation Biocatalysis and Bioseparation*, Vol. 5, (pp. 2379-2406). New York: Wiley.
- Chisti, Y. (2007). Biodiesel from microalgae. *Biotechnology Advances*, 25, 294-306.
- Chaumont, D. (1993). Biotechnology of algal biomass production: a review of systems for outdoor mass culture. *Journal of Applied Phycology*, 5, 593-604.

- Contreras, A., Garcia, F., Molina, E., & Merchuk, J.C. (1998). Interaction between CO₂-mass transfer light availability and hydrodynamic stress in the growth of *Phaedactylum tricorutum* in a concentric tube airlift photobioreactor. *Biotechnology and Bioengineering*, 60, 3, 317-325.
- Contreras, A., Garcia, F., Molina, E., & Merchuk, J.C. (1999). Influence of sparger on energy dissipation, shear rate, and mass transfer to sea water in a concentric-tube airlift bioreactor. *Enzyme and Microbial Technology*, 25, 820-830.
- Crippen, R.W., & Perrier, J.L. (1974). The use of neutral red and Evan's blue for live-dead determination of marine phytoplankton. *Stain Technology*, 49, 97-104.
- Degen, J. (2001). A novel airlift photobioreactor with baffles for improved light utilization through the flashing light effect. *Journal of Biotechnology*, 92, 89-94.
- Edwards, N., Beeton, S., Bull, A.T., & Merchuk, J.C. (1989). A novel device for the assessment of shear effects on suspended microbial cultures. *Applied Microbiology and Biotechnology*, 30, 190-195.
- Ewart, J.W., & Pruder, G.D. (1981). Comparative growth of *Isochrysis galbana* Parke and *Isochrysis aff galbana*, Clone T-ISO at four temperatures and three light intensities. *Journal of World Mariculture Society*, 12(1), 333-339.
- Garcia-Camacho, F., Contreras-Gomez, A., & Mazzuca-Sobczuk, T., et al. (2000). Effects of mechanical and hydrodynamic stress in agitated, sparged cultures of *Porphyridium cruentum*. *Process Biochemistry*, 35, 1045-1050.
- Garcia-Camacho, F., Molima-Grima, E. Sanchez-Miron, A., Gonzalez-Pascual, V., & Chisti, Y. (2001). Carboxymethyl cellulose protects algal cells against hydrodynamic stress. *Enzyme and Microbial Technology*, 29, 602-610.
- Gladue, R.M., & Maxey, J.E. (1994). Microalgal feeds for aquaculture. *Journal of Applied Phycology*, 6, 131-141.

- Goksan, T., Durmaz, Y., & Gokpinar, S. (2003). Effects of light path lengths and initial culture density on the cultivation of *Chaetoceros muelleri*. *Aquaculture*, 217, 431-436.
- Grobbelaar, J.U. (1994). Turbulence in algal mass cultures and the role of light/dark fluctuations. *Journal of Applied Phycology*, 6, 331-335.
- Gudin, C., & Chaumont, D. (1991). Cell fragility - the key problem of microalgae mass production in closed photobioreactors. *Bioresource Technology*, 38, 145-151.
- Guillard, R.L. & J.H. Ryther. (1962). Studies on marine planktonic diatoms. I. *Cyclotella nana* Hustedt and *Detinula confervacea* (Cleve). *Grand Canadian Journal of Microbiology*, 18, 229-239.
- Hu, Q. & Richmond, A. (1994). Optimizing the population density in *Isochrysis galbana* grown outdoors in a glass column photobioreactor. *Journal of Applied Phycology*, 6, 391-396.
- Janssen, M., Tramper, J., Mur, L.R., & Wijffels, R.H. (2002). Enclosed outdoor photobioreactors: light regime, photosynthetic efficiency, scale-up, and future prospects. *Biotechnology and Bioengineering*, 81, 193-211.
- Jaouen, P., Vandanjon, L., & Quemeneur, F. (1999). The shear stress of microalgal cell suspensions (*Tetraselmis suecica*) in tangential flow filtration systems: the role of pumps. *Bioresource Technology*, 68, 149-154.
- Kaplan, D., Cohen, Z., & Abeliovich, A. (1986). Optimal growth characteristics for *Isochrysis galbana*. *Biomass*, 9, 37-48.
- Kawase, Y., & Moo-Young, M. (1990). Mathematical models for design of bioreactors: Applications of Kolmogoro!'s theory of isotropic turbulence. *Chemical Engineering Journal*, 43, B19-B41.

- Kresta S. (1998). Turbulence in stirred tanks: Anisotropic, approximate and applied. *Canadian Journal of Chemical Engineering*, 76, 563–575.
- Krichnavaruk, S., Powtongsook, S., & Pavasant, P. (2007). Enhanced productivity of *Chaetoceros calcitrans* in airlift bioreactors. *Bioresource Technology*, 98, 2123-2130.
- Lange, H., Taillandier, P., & Riba, J. (2001). Effect of high shear stress on microbial viability. *Journal of Chemical Technology and Biotechnology*, 76, 501-505.
- Lee, Y.K., & Pirt, S.J. (1981). Energetics photosynthetic algal growth influence of intermittent-illumination in short (40s) cycles. *Journal of General Microbiology*, 124, 43-52.
- Lee, Y.K., Ding, S.Y., & Low, C.S. (1995). Design and performance of an alpha-type tubular photobioreactor for mass cultivation of microalgae. *Journal of Applied Phycology*, 7, 47-51.
- Lin, Y.H., Chang, F.L., Tsao, C.Y., & Leu, J.Y. (2007). Influence of growth phase and nutrient source on fatty acid composition of *Isochrysis galbana* CCMP 1324 in a batch photoreactor. *Biochemical Engineering Journal*, 37, 166-176.
- Liu, C.P., & Lin, L.P. (2001). Ultrastructural study and lipid formation of *Isochrysis galbana* CCMP1324. *A Quarterly Journal Containing Scientific Contributions from the Institute of Botany, Academia Sinica, Shanghai*, 42, 207-214.
- Merchuk, J.C. (1990). On the first order approximation to the response of dissolved oxygen electrodes for dynamic K_{La} estimation. *Biotechnology and Bioengineering*, 35, 1161-1163.
- Merchuk, J.C. (1991). Shear effects on suspended cells. *Advances in Biochemical Engineering*, 44, 64-94.

- Merchuk, J.C., Gluz, M., & Mukmenev, I. (2000). Comparison of photobioreactors for cultivation of the red microalga *Porphyridium* sp. *Journal of Chemical Technology and Biotechnology*, 75, 1119-1126.
- Molina-Grima, E., Chisti, Y., & Moo-Young, M. (1997). Characterization of shear rates in airlift bioreactors for animal cell culture. *Journal of Biotechnology*, 54, 195-210.
- Molina-Grima, E., Fernandez, J., Acien, F.G., & Chisti, Y. (2001). Tubular photobioreactor design for algal cultures. *Journal of Biotechnology*, 92, 113-131.
- Mueller-Fuega, A. (2000). The role of microalgae in aquaculture: situations and trends. *Journal of Applied Phycology*, 12, 527-534.
- Nelson, J.R., Guarda, S., Cowell, L.E., & Heffernan, P. (1992). Evaluation of microalgal clones for mass culture in a subtropical greenhouse bivalve hatchery: growth rates and biochemical composition at 30°C. *Aquaculture*, 106, 357–377.
- Park, K.H., & Lee, C.G. (2001). Effectiveness of flashing light for increasing photosynthetic efficiency of microalgal cultures over a critical density. *Biotechnology and Bioprocess Engineering*, 6, 189-193.
- Petersen, E.E., & Margaritis, A. (2001). Hydrodynamic and mass transfer characteristics of three-phase gaslift bioreactor systems. *Critical Reviews in Biotechnology*, 21, 4, 233-294.
- Pirt, S.L., Lee, Y.K., & Walach, M.R. (1983). A tubular bioreactor for photosynthetic production of biomass from carbon dioxide: design and performance. *Journal of Chemical Technology and Biotechnology*, 33B, 35–58.
- Pulz, O. (2001). Photobioreactors: production systems for phototrophic microorganisms. *Applied Microbiology and Biotechnology*, 57, 287-293.

- Qiang, H., & Richmond, A. (1994). Optimizing the population density in *Isochrysis galbana* grown outdoors in a glass column photobioreactor. *Journal of Applied Phycology*, 6, 391-396.
- Richmond, A., Boussiba, S., Vonshak, A., & Kopel, R. (1993). A new tubular reactor for mass production of microalgae outdoors. *Journal of Applied Phycology*, 5, 327-332.
- Richmond, A. & Cheng-Wu, Z. (2001). Optimization of a flat plate glass reactor for mass production of *Nannochloropsis* sp. outdoors. *Journal of Biotechnology*, 85, 259-269.
- Richmond, A. (2004). Principles for attaining maximal microalgal productivity in photobioreactors: an overview. *Hydrobiologia*, 512, 33-37.
- Sanchez-Miron, A., Contreras-Gomez, A., Garcia-Camacho, F., & Chisti, Y. (1999). Comparative evaluation of compact photobioreactors for large-scale monoculture of microalgae. *Journal of Biotechnology*, 70, 249-270.
- Sánchez-Mirón A., García-Camacho F., Contreras-Gómez A., Molina-Grima E., & Chisti, Y. (2000). Bubble column and airlift photobioreactors for algal culture. *AIChE Journal*, 46, 1872–1887.
- Sanchez-Miron, A., Ceron-Garcia, M.C., Contreras-Gomez, A., Garcia-Camacho, F., Molina-Grima, E., & Chisti, Y. (2003). Shear stress tolerance and biochemical characterization of *Phaeodactylum tricornutum* in quasi steady-state continuous culture in outdoor photobioreactors. *Biochemical Engineering Journal*, 16, 287-297.
- Sanchez-Perez, J.A., Rodriguez-Porcel, E.M., Casas-Lopez, J.L., Fernandez-Sevilla, J.M., & Chisti, Y. (2006). Shear rate in stirred tank and bubble column bioreactors. *Chemical Engineering Journal*, 124, 1-5.

- Silva, H.J., Cortinas, T., & Ertola, H.J. (1987). Effect of hydrodynamic stress on *Dunaliella* growth. *Journal of Chemical Technology and Biotechnology*, 40, 41-49.
- Suzuki, T., Matsuo, T., Ohtaguchi, K., & Koide, K. (1995). Gas-sparged bioreactors for CO₂ fixation by *Dunaliella tertiolecta*. *Journal of Chemical Technology and Biotechnology*, 62, 351-358.
- Talbot, P., Gonzales, M.P., Lencki, R.W., & de la Noue, J. (1991). Absorption of CO₂ in algal mass culture systems: a different characterization approach. *Biotechnology and Bioengineering*, 37, 834-842.
- Thomas, W.H., & Gibson, C.H. (1990). Effects of small-scale turbulence on microalgae. *Journal of Applied Phycology*, 2, 71-77.
- Timmons, M.B, & Ebeling, J.M., (2007). *Recirculating Aquaculture*. Ithaca, New York: Cayuga Aqua Ventures.
- Tramper, J., Williams, J.B., & Vlak, J.M. (1986). Shear sensitivity of insect cells in suspension. *Enzyme and Microbial Technology*, 8, 33-36.
- Tredici, M.R. (1999). Bioreactors, Photo. In: M.C. Flickinger and S.W. Drew (Eds.), *Encyclopedia of Bioprocess Technology: Fermentation Biocatalysis and Bioseparation. Vol. 1* (pp. 395-419). New York: Wiley.
- Tzovenis, I., De Pauw, N., & Sorgeloos, P. (2003). Optimisation of T-ISO biomass production rich in essential fatty acids. I. Effect of different light regimes on growth and biomass production.
- Ugwu, C.U., Ogbanna, J.C., & Tanaka, H. (2005). Light/dark cyclic movement of algal culture (*Synechocystis aquatilis*) in outdoor inclined tubular photobioreactor equipped with static mixers for efficient production of biomass. *Biotechnology Letters*, 27, 75-78.

- Vandanjon, L., Rossingnol, N., Jaouen, P., Robert, J.M., & Quemeneur, F. (1998). Effects of shear on two microalgae species. Contribution of pumps and valves in tangential flow filtration systems. *Biotechnology and Bioengineering*, *63*(1), 1-9.
- Wang, N.S., Yang, J.D., Calabrese, R.V., & Chang, K.C.(1994). Unified modeling framework of cell death due to bubbles in agitated and sparged bioreactors. *Journal of Biotechnology*, *33*, 107-1022.
- Watanabe, Y., & Hall, D.O. (1996). Photosynthetic production of the filamentous cyanobacterium *Spirulina platensis* in a cone-shaped helical tubular photobioreactor. *Applied Microbiology and Biotechnology*, *44*, 693-698.
- Weissman, J.C., Goebel, R.P., & Benemann, J.R. (1987). Photobioreactor design: mixing, carbon utilization, and oxygen accumulation. *Biotechnology and Bioengineering*, *31*, 336-344.
- Wikfors, G.H., & Ohno, M. (2001). Impact of algal research in aquaculture. *Journal of Phycology*, *37*, 968-974.
- Wu, J. (1995). Mechanisms of animal cell damage associated with gas by bubbles and cell protection by medium additives. *Journal of Biotechnology*, *43*, 81-94.
- Wu, X., & Merchuk, J.C. (2001). A model integrating fluid dynamics in photosynthesis and photoinhibition processes. *Chemical Engineering Science*, *56*, 3527-3538.
- Wu, X., & Merchuk, J.C. (2002). Simulation of algal growth in a bench-scale bubble column reactor. *Biotechnology and Bioengineering*, *80*, 2, 156-168.
- Xu, Z., Baicheng, Z., Yiping, Z., Zhaoling, C., Wei, C. & Fan, O. (2002). A simple and low-cost airlift photobioreactor for microalgal mass culture. *Biotechnology Letters*, *24*, 1767-1771.

Zhu, C.J., Lee, Y.K., & Chao, T.M. (1997). Effects of temperature and growth phase on lipid and biochemical composition of *Isochrysis galbana* TK1. *Journal of Applied Phycology*, 9, 451-457.